This article has been accepted for publication in IEEE Journal of Selected Topics in Applied Earth Observations and Remote Sensing. This is the author's version which has not been fully edited and content may change prior to final publication. Citation information: DOI 10.1109/JSTARS.2024.3362476

A Survey of Point Cloud Completion

Zhiyun Zhuang, Zhiyang Zhi, Ting Han, *Student Member, IEEE*, Yiping Chen, *Senior Member, IEEE*, Jun Chen, Cheng Wang, *Senior Member, IEEE*, Ming Cheng, *Member, IEEE*, Xinchang Zhang, Nannan Qin and Lingfei Ma, *Member, IEEE*

***Abstract*—Point cloud completion is able to estimate the complete point cloud starting from the missing point cloud, which obtains higher quality point cloud data for widely used in remote sensing 3D modeling, medical imaging, robot vision, etc. The challenge of point clouds mainly lies in the disordered and unstructured nature, which makes point cloud completion difficult. Point cloud completion research can be broadly categorized into traditional approaches and deep learning based methods. Recently, intensive research has primarily focused on deep learning based methods, given robustness and efficiency in processing the substantial missing data encountered in complex real world scenes. In addition, deep learning based methods have higher generalization performance. To stimulate future research, this survey presents a comprehensive review of existing traditional and deep learning based 3D point cloud completion methods. This review conducts extensive examinations of each stage of the process, providing a compilation of famous datasets, metrics, and their respective characteristics. Additionally, the impacts of subsequent downstream application tasks with or without completion are discussed, followed by some potential future issues in point cloud completion.**

***Index Terms*—point cloud completion, deep learning, 3D data, model construction, review**

I. Introduction

As a kind of 3D object format, point clouds have attracted more and more attention, which can express more realistic 3D geometry structure and spatial position of objects. Point clouds are acquired by 3D laser scanners, depth cameras and LiDAR (Light Detection And Ranging) sensors. However, due to the limitations in resolution and perspective of these sensors, as well as the occlusion and light reflection in the scanning process etc., the acquired point clouds is characterized by sparsity, incompleteness, and noise, which leads to the absence of some geometric and semantic information. The main reasons of missing point clouds is summarized in Table. I. More recently, advanced methods and impressive progress have been made in the classification and semantic segmentation of point cloud. However, these methods are usually designed for complete and clean point clouds, which are difficult to apply to the raw data obtained from low-cost sensors.

TABLE I
THE MAIN REASONS FOR MISSING POINT CLOUDS.

Reasons	Characteristic
Scan blind spot	Textures are complex in morphology
Missing details	Individual object point clouds are missing but repeatable
Occlusion by foreign objects	Textures are complex in morphology
Specular reflection	The surface texture is relatively single
The object is self-occluded	Simple surface texture and local features
Echo signal is absorbed	Complex geometry of objects

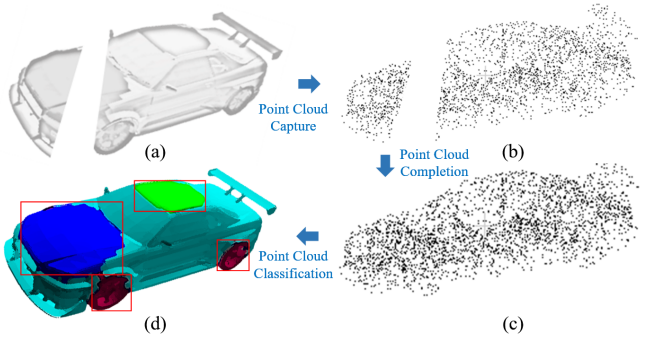


Fig. 1. The upstream and downstream of point cloud completion: (a) Objects obscured by other objects; (b) Disturbed object point clouds; (c) Point clouds that have undergone the complete algorithm; (d) The completed point cloud is used for the classification of different parts of the object.

Point cloud completion, also known as point cloud repair or 3D shape completion, involves the reconstruction and restoration of damaged or incomplete point clouds to generate a complete point cloud. Fig. 1 shows the upstream and downstream of point cloud completion. Point cloud completion plays an important role in the field of remote sensing, as shown in Fig. 2. Due to occlusion, low data quality, laser pulse penetration and incompleteness, point cloud surface models, buildings, forests, vegetation, and cultural heritages may exist incomplete data. Thus, point cloud completion can be used to generate more complete and more accurate surface models, the shape and height of buildings, forest parameters, cultural relics, and sparse point cloud completion in autonomous driving tasks. Improving the completeness and accuracy of point cloud is highly valuable for tasks such as extracting and inverting surface models, determining forest parameters, creating urban 3D models, detecting changes in buildings,

This work was supported by the National Natural Science Foundation of China under Project 42371343. *(Corresponding author: Yiping Chen)*

Z. Zhuang is with the College of Meteorology and Oceanography, National University of Defense Technology, Changsha 410073, China (e-mail: jy00842031@163.com).

Z. Zhi, T. Han, and Y. Chen are with the School of Geospatial Engineering and Science, Sun Yat-sen University, Zhuhai 519082, China (e-mail: zhizhy3@mail2.sysu.edu.cn, ting.devin.han@gmail.com, chenyp79@mail.sysu.edu.cn).

J. Chen, C. Wang, and M. Cheng are with the Fujian Key Laboratory of Sensing and Computing for Smart Cities, Xiamen University, Xiamen 361005, China (e-mail: chenjun97@stu.xmu.edu.cn, cwang@xmu.edu.cn, chm99@xmu.edu.cn).

X. Zhang is with the School of Geography and Remote Sensing, Guangzhou University, Guangzhou 510006, China (e-mail: zhangxc@gzhu.edu.cn).

N. Qin is with the School of Remote Sensing and Geomatics Engineering, Nanjing University of Information Science and Technology, Nanjing 210044, China (e-mail: 003689@nuist.edu.cn).

L. Ma is with the School of Statistics and Mathematics, Central University of Finance and Economics, Beijing 102206, China (e-mail: l53ma@cufe.edu.cn).

This work is licensed under a Creative Commons Attribution-NonCommercial-NoDerivatives 4.0 License. For more information, see https://creativecommons.org/licenses/by-nc-nd/4.0/

This article has been accepted for publication in IEEE Journal of Selected Topics in Applied Earth Observations and Remote Sensing. This is the author's version which has not been fully e
content may change prior to final publication. Citation information: DOI 10.1109/JSTARS.2024.3362476

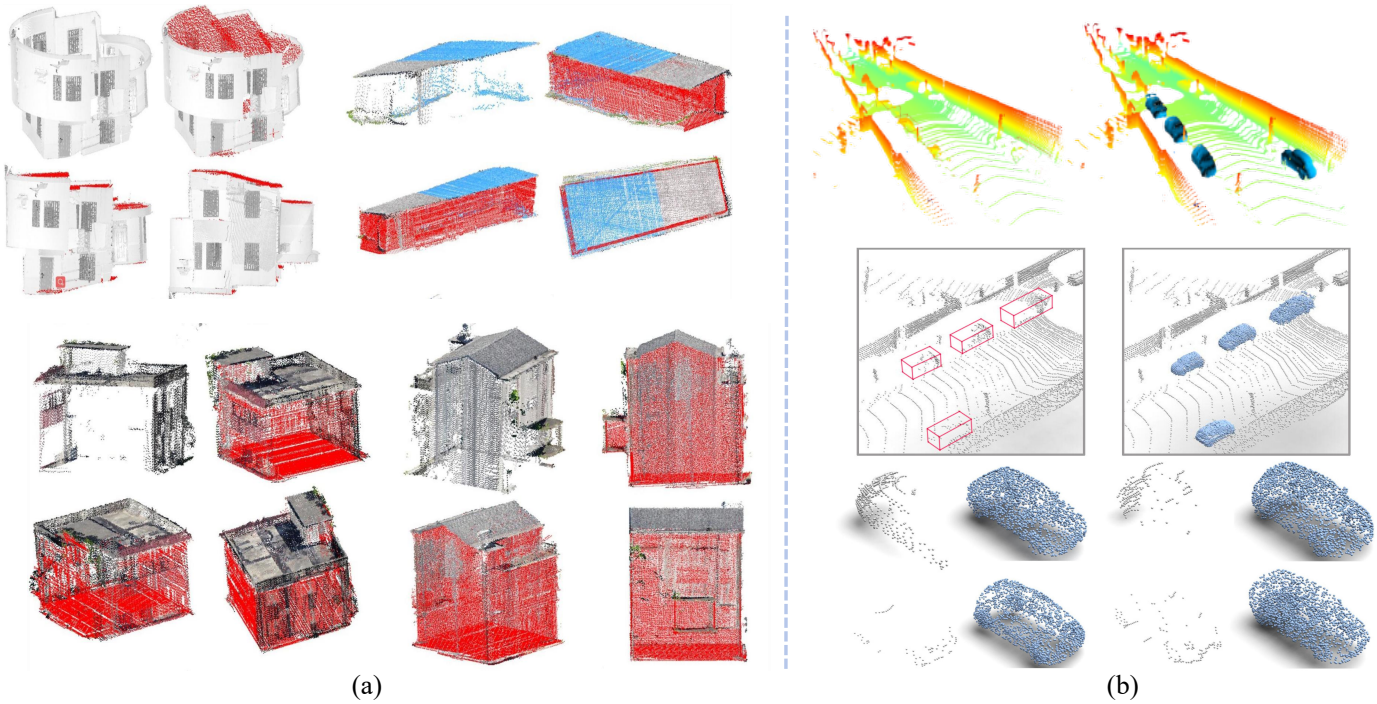


Fig. 2. The application of point cloud completion, where (a) represents the completion of building facades [1], and (b) sparse point cloud completion in autonomous driving [2].

monitoring forest ecology, and ensuring safety for advanced driver assistance systems.

In many autonomous driving tasks, LiDAR sensors are indispensable environmental sensing devices. Nevertheless, acquiring and processing the sensed external object data is an extremely challenging task. In Fig. 2(b), the gray objects indicate moving objects obtained by the sensor, but it is impossible to tell what the objects are due to limited shape attributes, and the blue parts are the complemented point cloud, which are cars with some probability and are compared with the actual objects detection (red boxes) to determine the accuracy of the completion algorithm.

Point cloud completion methods are primarily classified into traditional methods and deep learning based algorithms. The traditional methods is subdivided into geometric methods using geometric properties and alignment methods matching data models. However, traditional methods have limited completion effects due to the indeterminate lack of symmetry and rely heavily on model databases. Deep learning-based methods have become the current research trend. Early researchers focused on the conversion of data formats, which are mainly voxel-based methods, but such methods are greatly affected by resolutions. The existing point cloud completion methods are shown in Fig. 3. In addition, Fig. 4 illustrates some classical point cloud completion methods and how the number of related papers has changed over the last five years, where different colors represent different theoretical bases. After PointNet [4] and PointNet++ [5] were put forward, point-based methods have received the most attention. The number of papers published on point cloud completion is increasing, and the number of papers published in 2021 and 2022 both exceed 200. It shows that the research on point cloud completion is still at a high level of enthusiasm. Different models and methods are continuously proposed by researchers, among which point-based methods occupy the majority of the percentage.

In this survey, our contributions are as follows: (a) To the best of our knowledge, it is the first survey in the literature that interviews both the traditional and Deep learning-based approaches for point cloud completion. (b) We fully discuss both traditional and Deep learning-based point cloud completion methods. To provide a more comprehensive context for point cloud completion, we have made a comprehensive review from the geometric view of traditional methods to point-based neural networks and adversarial neural networks-based point cloud completion. (c) This paper encompasses the most recent advanced work with state-of-the-art methods. (d) This paper provides the analysis the comparative summary of divergent deep learning based researches and the conclusion about the trend of point cloud completion.

The remainder of this paper is structured as follows. Section II describes the current research challenges. A comprehensive survey of the existing traditional approaches and deep learning algorithms for 3D point cloud completion is provided in Section III, respectively. Evaluation of point clouds shape completion and some classical datasets are illustrated in Section IV. Moreover, the applications of point cloud completion in 3D vision tasks are presented in Section V. Finally, Section VI and Section VII discuss the future research trends and provide a conclusion for the survey.

II. Challenge

The completion operation takes incomplete data as inputs and aims to generate complete point clouds. Owing to the

This work is licensed under a Creative Commons Attribution-NonCommercial-NoDerivatives 4.0 License. For more information, see https://creativecommons.org/licenses/by-nc-nd/4.0/

This article has been accepted for publication in IEEE Journal of Selected Topics in Applied Earth Observations and Remote Sensing. This is the author's version which has not been fully edited content may change prior to final publication. Citation information: DOI 10.1109/JSTARS.2024.3362476

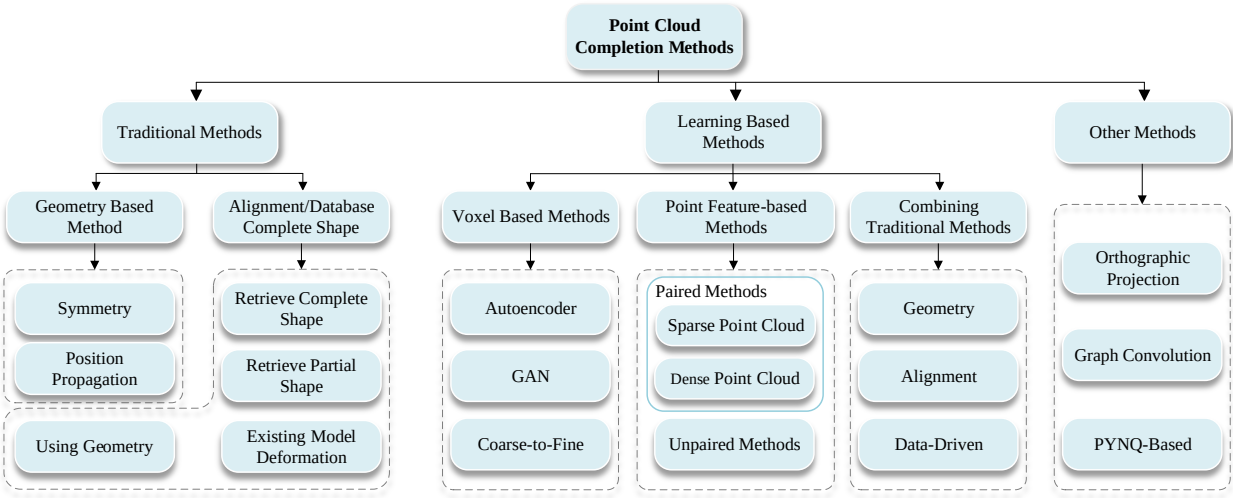


Fig. 3. Point cloud completion methods

absence of geometric and semantic information in incomplete point clouds, existing approaches suffer from the following challenges:

1) Low resolution original data to high resolution outputs and improvement. On one hand, many networks generate a point cloud of 2048 points, hence the completion effect in detail is not ideal enough. Generating a higher-resolution point cloud can improve the fine-grained details of the local object. On the other hand, the network architecture typically governs the resolution of the output point cloud. For different requirements, we need to generate specific resolutions [6].
2) Keep the overall shape and local details accuracy and uniformity. The network needs to be imaginative to infer the overall shape from the local clues. The inferred shape can contain multiple possibilities. In terms of local details, the detailed structure of partial inputs should be retained, and the generated local details should be as accurate as possible and free from noise points [7].
3) Large degree of missing input point clouds to intact point clouds. Many networks can be used as a parameterized model to learn the mapping between two potential spaces, i.e., incomplete point clouds and complete point clouds. However, in the case of highly incomplete remote sensing observed point clouds, the unstructured and sparse characteristics of point clouds make it challenging to distinguish between spatial blanks caused by sparsity or incompleteness. This predicament complicates the learning process when relies solely on single-modal point clouds [8].
4) Complex deficiency for poor generalization. Most point cloud completion methods rely to a large extent on paired incomplete-complete point clouds and adopt a fully supervised learning approach. Despite their impressive performance on intra-domain data, when generalized to various absences and forms of defective clouds or incomplete scans in the real world, satisfactory results are often not obtained due to remote sensing domain differences [9].
5) Real-time and time lineless requirements. In some applications, point cloud completion needs to be performed under real-time or near-real-time conditions. For instance, self-driving cars require the instantaneous perception and processing of point clouds within their surroundings.
6) Inadequate point cloud completion evaluation metric. Commonly used evaluation metrics include Chamfer Distance (CD) and Earth Mover's Distance (EMD). While CD is prone to uneven density distribution and unclear details, EMD exhibits greater sensitivity to details and density distribution. However, EMD's high computational cost makes it unsuitable for dense point clouds [10].

III. Methods

As illustrated in Fig. 3, three primary methods are commonly employed in point cloud completion, i.e., traditional methods, deep learning-based methods, and other methods. Furthermore, the timeline based on the most relevant method of point cloud completion is presented in Fig. 4, demonstrating the prevalent use of deep learning-based methods in current practices.

A. Traditional Methods

1) Geometry-Based Methods: Geometry-based methods basically leverage the geometric clues of missing input data to infer the shape of the missing part without any external auxiliary data for completing the overall shape of the data model.

Geometry-based methods leverage the geometric clues of missing input data to infer the shape of the missing part without any external auxiliary data for completing the overall shape of the data model. At the beginning of the research, many researchers paid attention to the small hole filling of the 3D model. Kazhdan et al. [11] proposed an algorithm for Poisson surface reconstruction. This algorithm utilized an

This work is licensed under a Creative Commons Attribution-NonCommercial-NoDerivatives 4.0 License. For more information, see https://creativecommons.org/licenses/by-nc-nd/4.0/

This article has been accepted for publication in IEEE Journal of Selected Topics in Applied Earth Observations and Remote Sensing. This is the author's version which has not been fully edited and content may change prior to final publication. Citation information: DOI 10.1109/JSTARS.2024.3362476

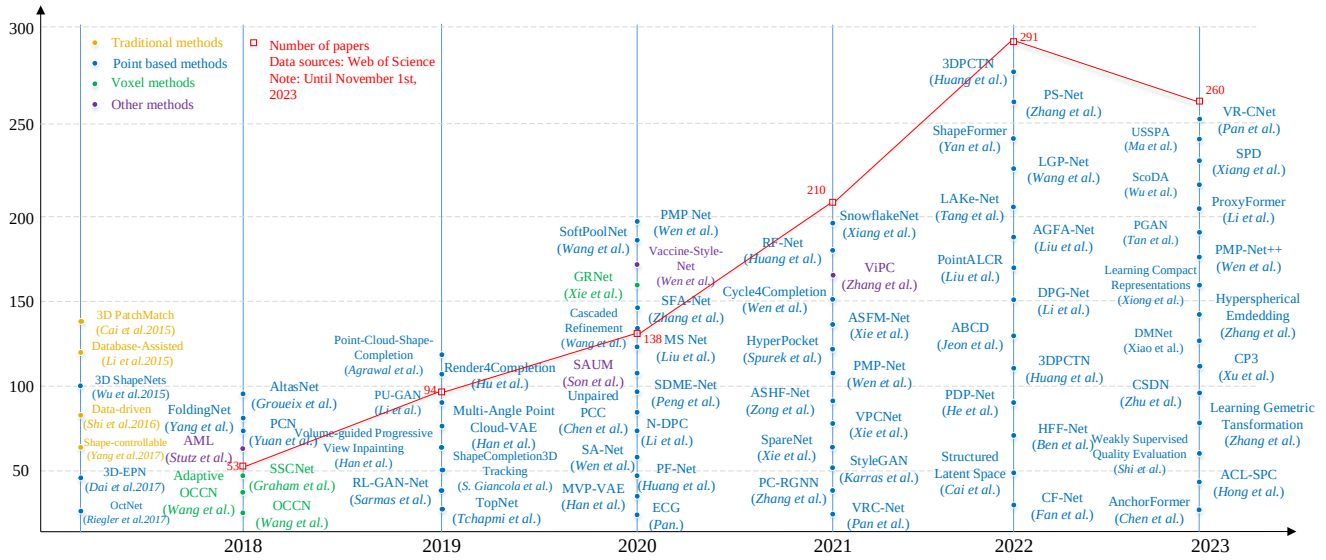


Fig. 4. Temporal overview of the most relevant point cloud shape completion methods.

implicit fitting method, amalgamating the advantages of global and local fitting and transformed the surface shape completion based on directional points into a Poisson problem for solving, whose spatial and temporal complexity was proportional to the size of the reconstructed surface. This algorithm can get a smoother surface and approach the noisy data robustly. Subsequently, Kazhdan et al. [12] proposed the shielded Poisson surface reconstruction algorithm, which selected a subset of sparse points, rather than the entire domain. Based on the original Poisson surface reconstruction algorithm, it incorporated the interpolation constraints into the input point cloud, resulting in the transformation of the original equation into the shielded Poisson. Zhao et al. [13] proposed a method to fill the holes in the triangular mesh model. First, they used the Advancing Front Mesh (AFM) to create a new triangle to cover the hole and estimate its normal. Then, according to the normal and the hole boundary vertices, the grid coordinates of the missing part were recalculated by solving the Poisson equation. Focusing on point cloud models, Yang et al. [14] designed a shape-controllable geometric completion algorithm based on the physical diffusion model. This method broke down the boundary contraction of each hole into two consecutive stages: normal propagation and position sampling. It incorporated normal dissimilarity constraints to fill the holes with obvious characteristics. These two stages were alternately applied until boundaries were formed without new holes. This approach provided potential shape selections for regions that might include sharp features. For point cloud completion, it is also necessary to consider the optimal matching time of searching the complete region to the cavity region. Therefore, Cai et al. [15] proposed a 3DPatchMatch algorithm to optimize the point cloud completion search process and quickly find the good match. This algorithm employed point clouds consistency to reduce convergence time through a process of random initialization and propagation. Furthermore, they proposed a random gaussian process to ensure the algorithm's ability to move away from local minima. Similarly, this method was suitable for smaller holes with reduced matching time. These methods are able to deal with relatively small hole deletions and usually hard to repair larger missing areas.

In order to fill the relatively larger missing area, some methods explore the shape completion of the 3D model of a specific shape category composed of basic primitives. Schnabel et al. [16] assumed that the 3D model comprised fundamental geometric primitives such as planes, cylinders, and cones. These primitives were employed to identify missing information within the input point cloud, facilitating the automated inference of the complete structure of the absent 3D model. Li et al. [17] further considered the geometric relationships among the orientations, positions, and equality of the primitives during the reconstruction process, and then designed a RANSAC [18] based algorithm to obtain the basic primitives for local fitting to gradually learned the relations among basic primitives and modified the model. For 3D model formed by interlacing curved tube structures such as coils and metal wires. Li et al. [19] presented the arterial-snake deformation model, which obtained the model topology and geometric structure from the missing input point cloud that contained noise to further realize shape completion. Although the above methods have achieved good results in some special and large missing 3D models, they are limited to models composed of specific basic primitives and have no general applicability.

Symmetry is one of the main features in traditional completion methods. Many objects have symmetry or partial regional symmetry [20]. In broader terms, symmetry can be identified even from a partial 3D view of a 3D model. This symmetry can be utilized to extend the visible regions of the 3D model into the occluded space, enabling the prediction of the shape of the missing components. Thrun et al. [21]

This work is licensed under a Creative Commons Attribution-NonCommercial-NoDerivatives 4.0 License. For more information, see https://creativecommons.org/licenses/by-nc-nd/4.0/

This article has been accepted for publication in IEEE Journal of Selected Topics in Applied Earth Observations and Remote Sensing. This is the author's version which has not been fully e
content may change prior to final publication. Citation information: DOI 10.1109/JSTARS.2024.3362476

proposed a symmetry search in the process of hierarchical generation and testing. This process interweaved the search in the symmetry type space with the search for specific symmetry parameters, and also divided the 3D model into sub-regions with different symmetries. The shape completion is achieved by using the symmetries of the local regions while limited to special eight types of objects. Mitra et al. [22] proposed a descriptor that described the local feature information of a 3D model. By calculating the local features of different regions, potential matching pairs were obtained, and then a random clustering algorithm was used to decide to find the local symmetry or approximate symmetry of the object to realize the shape completion. This method has versatile applications in geometry processing. Pauly et al. [23] proposed an algorithm framework for discovering regular or repeated geometric structures in 3D models. By analyzing paired similar transformations, the authors found prominent lattice structures such as rotation, translation, scaling, and symmetry to fill the missing areas. However, this method struggled with processing group data. Zheng et al. [24] focused on the field of large-scale urban architecture. They further integrated and complemented scanning data by detecting the common repeated geometric structures in the building scanning point clouds. Nevertheless, handling data quality and noise remains challenging. Sipiran et al. [25] generated the candidate symmetry by matching the local maximum value of the surface function based on the local thermal diffusion. They then utilized a voting method to detect symmetries within the 3D model. This approach only utilized symmetries with respect to planes instead of axes. Speciale et al. [26] proposed a method to detect multiple symmetries containing overlapping support regions. In this method, regions belonging to different symmetries were partially shared and symmetric prior information was used for completion. The advance is the ability to handle noisy objects. The above method relies on the symmetry of the data model itself, and this property is not only the matching of the visible area with other visible areas, but also the effective completion can only be achieved by the law associated with the blank region.

The advantages of geometry-based methods include their capacity to achieve shape completion through simple algorithms and perform well in a specific 3D model. However, these methods still have challenges with high requirements for the structure of the missing input models and the integrity scale of input data. The degree of completeness requires the shape and structure of the missing input model to be complete for estimating the shape of the missing region by using the existing clues. Restoring completion becomes challenging when a large number of models are missing. Additionally, geometry-based algorithms exhibit relatively low generalization performance when the geometric shape of the 3D model differs significantly. The solution for solving this problem requires different completion algorithms to be constructed, which leads to high computational costs to apply to large-scale point clouds.

2) Alignment-Based Methods: The basic idea of the alignment-based matching method (also known as the database-based method) is to retrieve and match the same or similar shape as the missing input model in the 3D shape database and replace the missing input data to complete the shape completion.

Simple completion algorithms can be replaced by directly retrieving the complete shape corresponding to the input model in the database. Nan et al. [27] presented a completion algorithm for scanned indoor scene data. Firstly, the search-classify method was used to find object instances with semantic information in the scanned point clouds. Then the model of the same category in the 3D shape database was used to match the object instance and replace the scan data. Li et al. [28] introduced a completion algorithm for real-time object retrieval in an environmental 3D shape database. This method used model key points and a 3D shape descriptor that integrated local and global information to search and match in the database, and replaced the scanned RGB-D data with the complete model in the 3D shape database. The algorithm realized object retrieval in the interactive scanning environment and allowed for online querying of a database containing thousands of models during the scanning process. Shi et al. [29] provided a data-driven method to model contextual information, which covered the relationship between parts within an object and the layout between objects. The algorithm integrated the detection of individual objects and object groups into a unified framework, eliminating the need for prior knowledge of objects within the scene. However, these methods are constrained by the assumption that the 3D shape database includes the same (or extremely similar) shape as the input model and are not easily generalized to new shapes.

To address this limitation, one potential approach was to initially retrieve shapes that closely resemble the input data from the 3D shape database. The matching model was deformed to more closely resemble the input missing data model. The models retrieved in this model did not have to exactly match the input data, so even a small database can cover a wider range of input data types. For example, Pauly et al. [30] proposed to retrieve candidate models similar to the input data from the 3D shape database followed by a non-rigid alignment between the input data and the candidate model to further complete the shape completion. This algorithm defined the shape-matching penalty function and the corresponding optimization scheme, which was used to calculate the non-rigid alignment of different candidate models and input data, and provided a quantitative comparison among different candidate models in order to select the best model. Rock et al. [30] designed a method for reconstructing a complete 3D model from a single depth map. The algorithm started by retrieving a matching 3D mesh model based on the depth map and subsequently deforming the candidate model to better align with the observed depth map. The deformation operation needs to conform to the symmetry of the input, and the final step involved combining the deformed model with the input to predict the complete shape of the target model. Gupta et al. [31] first performed feature detection and segmentation on the input data to obtain objects within the scanned scene. They then utilized the convolutional neural network (CNN) to estimate the rough pose of each detected object. Subsequently, the candidate models were aligned with the input objects from the 3D shape database, and the algorithm searched for the best-

This work is licensed under a Creative Commons Attribution-NonCommercial-NoDerivatives 4.0 License. For more information, see https://creativecommons.org/licenses/by-nc-nd/4.0/

This article has been accepted for publication in IEEE Journal of Selected Topics in Applied Earth Observations and Remote Sensing. This is the author's version which has not been fully edited and content may change prior to final publication. Citation information: DOI 10.1109/JSTARS.2024.3362476

fitting model that corresponded to the input data. Finally, the algorithm replaced the object in the scanned scene with the matching model from the database. Li et al. [32] introduced a method to reconstruct a 3D model from RGB-D by combining technologies based on contextual information and database templates. For the given input data, they calculated the non-rigid alignment between the candidate model from the same category in the 3D shape database and the input data. The candidate model with the best alignment was selected as the initial model, and a volumetric-patch-based algorithm was applied to further optimize the initial model, making it closer to the input data. Although the above methods have expanded the types of objects that can be matched by the 3D shape database to a certain extent, when the input data and the model in the database differ greatly, the cost and difficulty of designing a matching model deformation algorithm are greater.

In addition, some researchers [33], [34] built 3D shape database composed of basic parts, searched for matching parts in the database, and combined them to obtain a complex overall model to achieve completion. Shen et al. [33] proposed a bottom-up structural restoration algorithm based on parts assembly, which quickly converted low-quality point clouds obtained from consumer-level scanning equipment with corresponding RGB images into high-quality 3D models composed of different parts. The algorithm divided all data models in the 3D shape database into parts with different labels, retrieved parts that matched the 3D scan data and certain areas of the corresponding image in the database, and assembled them to obtain complete model. Sung et al. [34] used the symmetry of the data model and the part database to perform the shape completion. Simultaneously, this algorithm integrated data-driven technology to complete the structure and the shape of the missing point clouds. In contrast to the previous methods, which relied on the global coordinate system, the algorithm established the local coordinate system for each part, detected the position and orientation of the database part, and then joint optimization of all parts to find the most reasonable layout. Although the above part combination methods greatly expand the potential model space, it is necessary to accurately segment and mark each shape in the database. In addition, for input data with complex structures, the above methods may struggle to discover the global optimal solution due to the vast solution space. The alignment-based matching method relies on the huge number of models in the 3D shape database and the rich model types. The higher matching degree between the database model and the missing input data are, the better the completion effect.

B. Learning-Based Methods

Research on point cloud completion using deep learning can be mainly categorized into voxel-based and point-based methods. The graph-based, GAN-based, and Transformer-based methods are available as point-wise methods. Furthermore, we analyze point-wise methods by describing the processes based on the density and symmetry of the point cloud.

1) Voxel-Based Methods: The voxel-based method entails the voxelization of the disordered point cloud, followed by the use of the voxelized 3D model to accomplish shape completion. Voxelized point clouds is more suitable for leveraging CNNs for shape completion. Accordingly, Wu et al. [35] introduced 3D ShapeNets, a framework that utilized a Convolutional Deep Belief Network (CDBN) to model 3D geometric shapes as the probability distributions of binary variables on a 3D voxel grid. 3D ShapeNets learned complex 3D shape distributions across different categories and arbitrary poses, enabling 3D shape reconstruction based on depth maps. Nguyen et al. [36] proposed a method of using geometric data and multi-view RGB data to repair 3D shapes. This method modeled 3D shapes in Markov Random Field (MRF), and used CBDN in 3D ShapeNets to learn and represent local geometric information from a 3D shape database. Appearance information was then obtained from RGB images captured from multiple viewpoints, transforming the problem of incomplete shape completion into a Maximum A Posterior Probability (MAP) estimation within the MRF model. Han et al. [37] presented a completion algorithm combining global structural information with local geometric information, which consisted of two parts: a global structural inference network and a local geometric fine-tuning network. The global structure inference network adopted LSTM-CF [38] to predict the overall shape structure of the original data. Further, it enriched the global structure information by using a 3D full convolution (3DFCN) module. Dai et al. [39] proposed the algorithm 3D-EPN for voxel-based CNN and 3D shape synthesis. The algorithm first extracted feature information from the input model using the structure of 3D CNN and fused the semantic information obtained from a classification network to obtain a low-resolution rough point cloud. Subsequently, the whole data model associated with the rough point cloud was searched in the 3D shape database. Finally, the rough point cloud was further synthesized into the completion point cloud by combining with the matched complete data model.

To further account for the structure and context of point clouds, Xie et al. [40] proposed a Gridding Residual Network (GRNet). The method employed a 3D grid as the intermediary representation to standardize disordered point clouds. The transformation between point clouds and 3D grids can be realized without losing structural information, ensuring the network preserved the point cloud's structure and background. Wang et al. [41] designed a voxel-based network for point cloud completion, incorporating the edge generation (VE-PCN) to generate fine-grained details. They embed point clouds into regular voxel grids and generated complete objects by leveraging hallucinated shape edges. This decoupled architecture, along with a multi-scale grid feature learning, enabled the generation of more realistic on-surface details. These approaches usually conduct the convolution operation within a regular voxel grid, demanding high memory and computational costs, thus complicating the support for high-resolution input data. In order to reduce computational costs, some researchers began to explore the sparse voxel representations and the structural design of irregular convolution.

Riegler et al. [42] proposed the deep learning representation method OctNet based on sparse 3D data. The method took the advantage of the sparsity of point clouds, employing an

This work is licensed under a Creative Commons Attribution-NonCommercial-NoDerivatives 4.0 License. For more information, see https://creativecommons.org/licenses/by-nc-nd/4.0/

This article has been accepted for publication in IEEE Journal of Selected Topics in Applied Earth Observations and Remote Sensing. This is the author's version which has not been fully edited and content may change prior to final publication. Citation information: DOI 10.1109/JSTARS.2024.3362476

unbalanced octree to partition the space into layers. Each leaf node within the octree stored a pooled feature representation. This approach centralized memory allocation and computation in related dense areas, enabling deeper networking without compromising resolution. Wang et al. [43] proposed O-CNN. In this algorithm, the average normal vector stored in the leaf nodes of the octree was used as inputs for the CNN calculation. The operation of the CNNs was confined to the octree with 3D shape boundaries, which greatly reduced the computation cost. Wang and Sun et al. [44] proposed Adaptive O-CNN, a convolutional neural network based on adaptive octree. Different from traditional octree-based methods that used voxels of the same resolution to represent 3D shapes of data models, the Adaptive O-CNN algorithm used octrees at different levels and used a plane slice at each node to simulate 3D shapes, which reduced memory and computational overhead. In real scenes, many point clouds obtained by scanning are very sparse, and the standard dense implementation of CNN is very inefficient when applied to such sparse data. Graham et al. [45] proposed Submanifold Sparse Convolutional Networks (SSCN) for sparse data. The SSCN algorithm defined novel sparse convolution operations that effectively processed sparse data, enabling the implementation of spatial sparse convolution networks. These methods effectively reduce the time and space cost of computation and enable the model to process higher-resolution data. The voxel-based approach offers the advantage of drawing insights from well-established CNNs in the field of applied images. However, the calculation of the voxel format is large and the information is sparse. Despite remarkable advancements in 3D volume data research, the computational expenses, which are closely tied to input data resolution, pose challenges in handling intricate shapes.

2) Point Feature-based Methods: Point feature-based approaches leverage recent advances in DCNNs designed to work directly with point clouds. Notably, PointNet [4] and its extended network PointNet++ [5] are at the forefront in this field. These two network used multi-layer perceptrons to independently model each point and subsequently utilized symmetric functions to aggregate global features to achieve invariance to permutation and robustness to perturbation. Moreover, these two networks can be used as a model encoder to effectively extract features of disorderly point clouds. In this survey, we roughly divide these methods into paired training methods and unpaired point cloud completion methods. Furthermore, we divide the paired point cloud training methods into sparse completion and dense completion for a more detailed explanation.

a) Sparse Point Cloud Completion: Many existing methods focus on sparse point cloud completion, that is, the number of point clouds after completion does not exceed 2048. Yang et al. [46] proposed an end-to-end auto-encoder network FlodingNet. This network leveraged a graph-based encoder [47] to enhance the local structural features of PointNet. Subsequently, a folding-based decoder was designed to deform a canonical 2D mesh to a 3D smooth object surface. Wen et al. [48] proposed a point cloud completion network SA-Net to integrate the Skip-Attention mechanism. PointNet++ provided the backbone of the encoder to extract features. Under different resolutions, Skip-Attention was used to selectively transmit partial feature information of incomplete point clouds. The hierarchical decoder was employed to gradually refine the point clouds by layer folding, and then layers retained the complete structure of the point clouds at the corresponding resolution. These methods all adopt the architecture of the encoder and decoder to extract the characteristic information of point clouds and reconstruct the point cloud with the decoder.

In addition, many researches introduced Generative Adversarial Networks (GANs) into the sparse point cloud completion. Achlioptas et al. [49] used a PointNet-based auto-encoder to learn the latent feature representation of point clouds. These features were trained in the potential feature space by GANs and remapped to generate 3D point clouds. The algorithm can perform shape completion to a certain degree, but the network structure is not designed for shape completion. The performance of the network decreases significantly when the number of input point cloud deletions increases. In order to connect the auto-encoder and the GAN trained in the latent feature space and complete the missing point clouds, Gurumurthy et al. [50] suggested an initialization encoder. However, for the input data, this algorithm spent much time finding the optimal noise input z of GAN. Sarmad et al. [51] proposed RL-GAN-Net, which was divided into three modules: auto-encoder, latent-space GAN (*l*-GAN), and reinforcement learning agent. First, an auto-encoder was trained to obtain the potential spatial representation of the point cloud. Then, the representation was used to train the GAN to obtain the new feature vector from the noise z passing through the generator. The reinforcement learning agent was used to reduce the selection time cost of noise input z. Unlike Gurumurthy et al. [50], this network found the correct vector z through back propagation.

The PF-NET proposed by Huang et al. [52] generated high-quality point clouds. It retained the spatial arrangement of the input incomplete point cloud and only predicted the geometric structure of the missing region, which was different from most methods that predicted the overall shape of the point cloud. PF-NET used a multi-scale generation network based on feature points to estimate the missing point cloud hierarchically, introduced a discriminator to evaluate the quality of the output point cloud, and added an adversarial loss to the loss function to generate a more realistic missing area. The SFA-Net [53] also conducted multi-scale feature extraction to address the issue of detail loss in the completion process. They proposed two feature aggregation strategies: global and local feature aggregation (GLFA) and residual feature aggregation (RFA). In addition, they also designed a refinement component to evenly distribute the reconstructed coordinates, while also reducing noise and outliers. Surek et al. [54] redefined the point cloud completion problem as an object hallucination task. They proposed the Hyperpocket architecture, which used an auto-encoder based on a hypernetwork paradigm design. This method generated several different possible point cloud completion results for the given point cloud, rather than a single reconstruction. Further, Zhao et al. [55] have employed PF-NET for sparse facade point cloud completion.

This work is licensed under a Creative Commons Attribution-NonCommercial-NoDerivatives 4.0 License. For more information, see https://creativecommons.org/licenses/by-nc-nd/4.0/

This article has been accepted for publication in IEEE Journal of Selected Topics in Applied Earth Observations and Remote Sensing. This is the author's version which has not been fully edited and content may change prior to final publication. Citation information: DOI 10.1109/JSTARS.2024.3362476

b) Dense Point Cloud Completion: Dense point clouds contain more detailed features. Yu et al. [56] first used deep neural networks to generate denser and more uniform point clouds from sparse point clouds. The method was a data-driven point cloud up-sampling technique. The core concept involved learning multi-level features in a point-wise manner and expanding the point set implicitly in feature space using a multi-branch convolution unit. The expanded feature was subsequently divided into multitude features, which were then reconstructed to an up-sampled point set. It is noted that the structure of point sets is irregular and the domain is not fixed, so it is usually time-consuming to use a K-neighborhood search. Similarly, the down-sampling operation in extracting features at different scales can lose some geometric details. As far as our knowledge goes, Yuan et al. [57] first proposed PCN algorithm for dense point cloud completion in 2018. After completion, the number of point clouds is 16,384, which is 8 times larger than that of 2,048 for sparse point clouds. PCN was based on the encoder-decoder architecture and used the strategy of coarse-to-fine. The encoder obtained the global feature vector of the point cloud using the extended network based on PointNet. Then the global feature vector achieved the shape completion of the dense point cloud through a two-stage decoder. In the first stage, fully connected (FC) layers and reshape operations were used to obtain rough point clouds. In the second stage, dense point clouds were formed by combining global feature vectors through the folding network. The algorithm combined the advantages of FC layers and FoldingNet. Then, Zhao et al. [58] continued to employ the FoldingNet for remote sensing point cloud completion.

Subsequently, Tchapmi et al. [59] proposed the point cloud completion algorithm TopNet in 2019. This algorithm used the encoder developed by Yuan et al. [57], but the decoder adopted a hierarchical tree structure, so there was no need to set any topological structure for the input point set, and the completion task was capable of multi-resolution. The root node of the decoder stored the global feature vector obtained by the encoder, and then the multilayer perceptron was used to regress the coordinate value of the point cloud. Although PCN and TopNet complete point cloud completion to a certain extent, the object details are difficult to reconstruct. In order to obtain high-fidelity dense point cloud and avoid uneven distribution, blurred details as well as loss of structure in the results of the existing methods, many improvements have been made in subsequent methods. Li et al. [57] proposed N-DPC that was based on the structure of PCN. Self-attention unit was used for encoding to extract global features with more information, and then combined with local features to realize dense point cloud completion.

Peng et al. [60] introduced SDME-Net, which was designed for uniform completion of unstructured point clouds. The network was a two-stage multi-encoder architecture that used the coarse-to-fine strategy similar to that in the PCN. It first generated a complete sparse point cloud and then generated a dense point cloud. In addition, they used repulsion loss to ensure a more uniformly distributed output. Wang et al. [61] proposed a cascade algorithm and adopted the strategy of coarse-to-fine to synthesize dense point clouds based on GAN. The generator based on the encoder-decoder synthesized the local and global information of the missing point cloud to generate high-quality data completion. The discriminant distinguished the completion point cloud and the target point cloud is obtained by the generator. In order to obtain a better completion effect, the loss function of this algorithm combined the loss of conventional GAN and the structural loss of the completion point cloud and the target point cloud. Cheng et al. [62] designed two GAN-based modules to translate point cloud into partition. DPCG-Net is able to capture the global feature distributions and calculate the similarity between the regenerated global feature and the ground truth. This method significantly reduces the missing in cases where the lack of a large proportion of point clouds results in a large loss of spatial structure. Most GAN-based works fail to deal with diverse corrupted point cloud with large missing areas. Zhang et al. [63] proposed quasi-immune architecture, which is inspired by the artificial immunization process in biology. It transforms point cloud to surfaces with a continuous decision boundary function, while deduces complete surface from corrupted point cloud by the cooperation of reinforcement learning and latent GAN.

The MSNet [10] also used the basic idea of coarse-to-fine. The first step was to predict the coarse-grained point cloud from inputs. The second step combined the prediction with the original input, and used density sampling to obtain a uniformly distributed point cloud subset. Then it learned the point cloud residuals to obtain fine-grained details. This method preserved the structure of the object and produced details that were continuous and smooth. The ECG [64] proposed by Pan et al. is based on the coarse-to-fine strategy. This method formed a skeleton to capture the edge features, and then used the deep hierarchical encoder with graph convolution to make use of the features, so as to achieve the refinement of local geometric details. The MAP-VAE proposed by Han et al. [65] incorporated a multi-angle analysis of point cloud for effective local self-supervised feature learning, combining it with global self-supervision under variational constraints to complete more local geometric details. Xie et al. [7] proposed SpareNet, which used a style-based adversarial rendering point generator for point cloud completion. This framework used channel-attentive Edge-Convs to combine local and global contexts in point feature extraction. Styles-based folding was also used to enhance point cloud synthesis capability. In addition, adversarial point rendering was used to capture the geometric details of the point cloud. Zong et al. [66] proposed an adaptive sampling and hierarchical folding network ASHF-Net for robust point cloud completion. In this network, a denoising encoder with an adaptive sampling operation was used to learn local features which are not sensitive to noise. Then a layered folding encoder with gated skip attention and multi-resolution target completion was used to exploit these local structural details.

Xia et al. [67] proposed ASFM-NET based on feature matching of partial point clouds and complete point clouds. An asymmetric Siamese auto-encoder network was designed to infer missing geometric details using shape prior and iterative refinement units. The SoftPoolNet proposed by Wang

This work is licensed under a Creative Commons Attribution-NonCommercial-NoDerivatives 4.0 License. For more information, see https://creativecommons.org/licenses/by-nc-nd/4.0/

This article has been accepted for publication in IEEE Journal of Selected Topics in Applied Earth Observations and Remote Sensing. This is the author's version which has not been fully e
content may change prior to final publication. Citation information: DOI 10.1109/JSTARS.2024.3362476

et al [68] adopted a feature extraction method based on feature activation. In the decoding stage, the region convolution operator was used to maximize the global activation entropy. In addition, inspired by PCN, patch deformation was used to simulate point cloud deconvolution. This method can be integrated into many point cloud architectures, such as PCN, to improve the performance of geometric completion. Wen et al. [69] proposed PMP-Net, which expressed the predicted missing points as the deformation process of point clouds. This deformation was different from the complete deformation such as folding, but the point cloud completion was realized by moving every point in the incomplete input. Based on the constraint that the total distance of point movement is the shortest, the network predicted the movement path of each point and captured the detailed topological relationship between the incomplete shape and the complete object. Strict and unique correspondence was learned at the point level, thereby improving the quality of the predicted complete shape. Subsequently, PMP-Net++ [70] similarly mimicked behavior of earth mover to record the point cloud deformation process, moving incomplete point clouds to acquire the complete shape. Pan et al. [71], [72] proposed VRCNet, which was composed of a cascade of the probabilistic model network (PMNet) and relationship enhancement network (RENet). PMNet used global features and distribution of point cloud to generate a rough global framework structure, and then RENet enhanced the generation of relational shape details. To address the challenge of revealing fine local geometric details on the complete shape, Xiang et al. [73], [74] introduced SnowflakeNet with Snowflake Point Deconvolution (SPD) for generating complete point clouds. The SnowflakeNet regarded the generation of complete point clouds as a process resembling the growth of snowflakelike in 3D space, where child points were progressively generated by splitting from their parent points after each SPD operation. Our key insight of revealing intricate geometry involves incorporating a skip-transformer within SPD to learn point-splitting patterns for local regions.

c) Unpaired Point Cloud Completion: The unpair method refers to the training process of 3D point cloud completion without knowing the correspondence between complete and incomplete shapes, which can eventually predict the complete 3D shapes from incomplete inputs.

Inspired by the work of Achlioptas et al. [49], Chen et al. [75] proposed a shape completion algorithm that used unpaired data for training. The GAN was designed to transition between two different potential spaces, performing unpaired shape completion in real scans. In the global feature vector space, the algorithm used unpaired data to train against and generate networks, which can be well applied to the real scene scanning data. However, the algorithm only paid attention to learning geometric correspondence from incomplete to complete shapes while neglecting learning in the opposite direction, which leads to the limited ability of the algorithm to understand 3D shapes. Liu et al. [76] proposed the AGFA-Net combining spatial and channel attention blocks to selectively convey geometric features from local regions of partial point clouds to the completion process. Wen et al. [3] proposed Cycle4Completion, an unpaired point cloud completion network, to establish bidirectional geometric correspondence between incomplete and complete shapes, so as to further improve the completion performance.

Zhang et al. [9] focused on the generalization of different partial shape forms and proposed a novel unpaired shape completion network ShapeInversion. It employed a GAN pretrained on complete shapes to search for a latent code that yielded the best reconstruction of the given partial input as a complete shape. This approach gave robust results for real-world scans and partial inputs of varying forms and levels of incompleteness. However, its results were often uneven because of the excessive attention on the partial input, and it took a long time to infer a complete shape due to latent code searching. The PGAN proposed by Tan et al. [77] learned the local structure of incomplete point clouds and the global shape through a multi-scale generation module, and then employed adversarial training to analyze the geometric shape of point clouds.

To establish the correspondence between two data patterns, the previous approach employed adversarial training to match global shape features extracted by the encoder. However, this process neglected the correspondence between the multi-scale geometric information embedded within the decoder pyramid hierarchy. Cao et al. [78] proposed a novel unpaired shape completion network MFM-Net, which used multilevel feature matching to create multiple feature channels at different layers of the decoder using a dual-path architecture to enhance the understanding of 3D shapes. By combining this with the adversarial learning to merge the feature distribution from both complete and incomplete modalities, the learning of corresponding geometry in the point cloud decoder is deconstructed into a multilevel generative process. Zhang et al. [79] proposed multi-resolution encoder to extract and fuse multi-scale features avoiding information loss. And then, they employed multi-resolution point cloud generation structure, combining the encoder to generate generally dense point cloud. Xiong et al. [80] aligned sparse point cloud representations with dense point clouds and generates diverse, realistic dense point clouds by learning the prior information of discrete codebook.

C. Other Methods

The SAUM proposed by Son et al. [81] combined traditional methods. This method improved shape fidelity, especially for narrow fine structures. The whole network consisted of two complementary prediction branches. One branch learned global semantics from the database model and compensated for existing details. This branch can also be replaced by other traditional methods. Another branch Symmetry-Aware Up-sampling Module (SAUM) used fine structure and symmetry of partial observations to complete the shape. SAUM was easily combined with existing encoder-decoder structure completion methods. Yan et al. [6] proposed Vaccine-Style-Net, which was completed in the functional space of 3D surfaces. This approach cannot directly handle the point cloud, but rather infer the underlying continuous 3D shape from the discrete point cloud. It then incorporated a reinforcement

This work is licensed under a Creative Commons Attribution-NonCommercial-NoDerivatives 4.0 License. For more information, see https://creativecommons.org/licenses/by-nc-nd/4.0/

This article has been accepted for publication in IEEE Journal of Selected Topics in Applied Earth Observations and Remote Sensing. This is the author's version which has not been fully edited and content may change prior to final publication. Citation information: DOI 10.1109/JSTARS.2024.3362476

learning agent to generate complete output from incomplete point cloud. This represented an indirect method of shape completion. The completion process occurred within the latent space of 3D shapes, and due to the continuous representation, the output resolution was arbitrary.

Due to the large degree of point cloud missing, there is a huge challenge in learning mapping from the incomplete point cloud to the complete point cloud. Zhang et al. [8] proposed ViPC, which was different from the method of directly inferring missing points using shape priors. Instead, ViPC introduced a view-guided point cloud completion approach to extract essential missing global structural information from additional single-view images. In practice, fully supervised learning may not be available. Therefore, Stutz et al. [82] proposed a 3D shape completion method AML (amortized maximum likelihood) based on weak learning. It first used a variational auto-encoder to acquire shape-prior information from synthetic data and subsequently trained a new encoder to embed observations into the same latent space utilizing unsupervised maximum likelihood loss, thereby achieving shape completion without sacrificing accuracy.

PoinTr proposed by Yu et al. [83] reformulated point cloud completion as a set-to-set translation problem. Based on the 3D geometry-aware block that models the local geometric relationships, Transformer learned better structural knowledge and preserved detailed information for point cloud completion. Further, they developed an adaptive query generation mechanism and designed a novel denoising task during completing point cloud [84]. Coupling geometry-aware and adaptive query enabled model more efficient and effective. Zhou et al. [85] introduced SeedFormer to capture general structures from partial inputs and preserve regional information of local patterns. Wodzinski et al. [86] introduced an iterative, Transformer-based approach for reconstructing missing point clouds. However, unordered nature of point clouds degraded generation of high-quality 3D shapes. Chen et al. [87] had introduced a completion strategy based on anchors. This method leveraged pattern awareness to identify nodes using anchors and then dispersed these nodes into unobserved areas to dynamically capture object information. Li et al. [88] analyzed the relationship between features and positions in point clouds to represent missing points with existing ones. Then, it refined the missing points using a Transformer with position information generated from a normal distribution.

Zhu et al. [89] proposed a cross-modal shape refinement network that transferred image shape features for coarse predictions. It then refined the coarse output using point cloud positions, which included both global constraints and the ability to refine the geometric relationships of points locally. However, the spatial distribution of features was sparse. Therefore, Zhang et al. [90] proposed hyperspherical module to optimize feature orientation information. Zhang et al. [91] transformed point cloud completion into a geometric transformation problem by recovering the complete shape through the discovery of repetitive geometric structures.

Xu et al. [92] addressed the issues of (1) the lack of robustness in point cloud generation and (2) the absence of semantic awareness in the refinement stage by transforming the point cloud completion problem into self-supervised learning, resembling natural language prompts and predictions. Hong et al. [93] had proposed a self-supervised framework to overcome the differences between synthetic and real data. It utilized an adaptive closed-loop system to complete partial point clouds into complete point clouds. Subsequently, Shi et al. [94] introduced a weakly supervised point cloud completion evaluation network to optimize real data. Xiao et al. [95] proposed DMNet, as an unsupervised network, leveraged hierarchical-aware hyperbolic decoder to recover the point cloud shape based on semantic information discrimination. Wu et al. [96] proposed ScoDA to learn global and local knowledge between synthetic and real data. USSPA proposed by Ma et al. [97] is an unsupervised symmetric shape-preserving autoencoding network that refined features while simultaneously providing more detailed shape predictions.

IV. Evaluation of Point Cloud Completion

A. Datasets

At present, fourteen datasets are mainly used for point cloud completion research: i.e., synthetic 3D dataset ShapeNet [98], real world LiDAR dataset KITTI [99], PCN Dataset [57], and TUM-MLS-2016 [100] in remote sensing, as shown in Table. II. Their specific contents are described as follows:

1) Synthetic 3D Datasets:

a) **ShapeNet [98]:** A large repository of 3D CAD models with rich annotations. It includes more than 3 million models and provides a large number of semantic annotations for each model. The database divides 220,000 models hierarchically into 3,135 categories based on WordNet Synset. ShapeNet contains multiple subsets, of which ShapeNetCore has 55 common categories and approximately 51,300 single clean 3D models. This subset has manually verified categories and alignment annotations. Another subset, ShapeNetSem, has 270 categories and 12,000 models. This subset is smaller but has denser annotations. Compared to ShapeNetCore, it adds the labeling of real-world dimensions, the estimation of its material composition at the category level, and the estimation of its total volume and weight.

b) **ModelNet [35]:** To relieve the restriction of previous CAD datasets both in the variety of categories and the number of examples per category, Wu et al. constructed ModelNet, a large-scale 3D CAD model dataset. It is released in 2015 by the Princeton Vision and Robotics Laboratory to provide a comprehensive collection of clean 3D CAD models of objects for researchers in computer vision, computer graphics, robotics, and cognitive science. The dataset contains a total of 127,915 CAD models, 662 object categories, and 10 categories with annotated orientation. On one hand, 40 categories and 12,311 pre-aligned shapes are included in the ModelNet40 dataset, with 9,843 (80%) and 2,468 (20%) being used for training and testing respectively. ModelNet10, on the other hand, is part of ModelNet40 and is designed to build a more core dataset with manual alignment of orientation for a subset of CAD models of 10 popular object categories, containing 10 categories and 4,899 pre-aligned shapes, of which 3,991 (80%) and 908 (20%) are used for training and testing, respectively.

This work is licensed under a Creative Commons Attribution-NonCommercial-NoDerivatives 4.0 License. For more information, see https://creativecommons.org/licenses/by-nc-nd/4.0/

This article has been accepted for publication in IEEE Journal of Selected Topics in Applied Earth Observations and Remote Sensing. This is the author's version which has not been fully edited and content may change prior to final publication. Citation information: DOI 10.1109/JSTARS.2024.3362476

TABLE II
EXISTING PUBLIC POINT CLOUD COMPLETION DATASETS IN LIDAR REMOTE SENSING.

Dataset Name	Period	Type	Characteristic	Category	Representation
KITTI [99]	2012	Real-World	Urban, labeled, sparse, incomplete	8	Point Cloud
ShapeNetCore [98]	2015	Synthetic	Structured, labeled, low quality grid	55	Mesh
ShapeNetSem [98]	2015	Synthetic	Smaller and more densely annotated	270	Mesh
ModelNet10 [35]	2015	Synthetic	Part of ModelNet40	10	Mesh
ModelNet40 [35]	2015	Synthetic	Structured, labeled, simple structure	40	Mesh
TUM-MLS-2016 [100]	2016	Real-World	Urban, labeled, sparse, incomplete	8	Point Cloud
Semantic3D [101]	2017	Real-World	Outdoor, labeled; churches, streets to name just a few	8	Point Cloud
2D-3D-S dataset [102]	2017	Real-World	indoor, Registered modalities from 2D, 2.5D and 3D domains	-	Mesh
ScanNet [103]	2017	Real-World	Indoor, labeled, uneven, noisy and hollow	21	RGB-D
Matterport3D [104]	2017	Real-World	Indoor, labeled, uneven, noisy and hollow	40	RGB-D
PCN Dataset [57]	2018	Synthetic	Derived of ShapeNet	8	Mesh
Completion3D [59]	2019	Synthetic	Derived of ShapeNet	8	Mesh
Multi-View Partial Point Cloud (MVP) [71]	2021	Synthetic	With a different perspective	16	Point Cloud
ShapeNet-ViPC [8]	2021	Synthetic	Derived of ShapeNet	13	Mesh

c) **PCN [57]:** This dataset is a subset of the ShapeNet dataset used in PCN, which contains 8 categories of airplanes, cabinets, cars, chairs, lamps, sofa, tables, and vessels, with a total of 30,947 objects. The complete point cloud has 16,384 points, which are uniformly sampled from the grid model. Partial point clouds are generated by back-projecting of 2.5D depth images into 3D. Since this dataset is derived from a synthetic dataset, it contains complete objects, detailed 3D models, and exact ground truth values, making it more suitable for generating training data than real-world dataset.

d) **Completion3D [59]:** The Completion3D dataset includes 8 classes (Plane, Cabinet, Car, Chair, Lamp, Couch, Table, and Watercraft). It contains both partial and complete shapes, making it more suitable for research and development of 3D modeling and recognition tasks that require handling partial shapes. In contrast, other datasets only contain complete 3D shapes, thus cannot provide training and evaluation for handling partial shapes.

e) **Multi-View Partial (MVP) Point Cloud Dataset [71]:** The Multi-View Section (MVP) point cloud dataset contains point clouds acquired on a unit sphere using 26 evenly distributed camera poses. At the same time, the dataset compares rendered incomplete point clouds with different camera resolutions. The resulting dataset is tested, and the results show that the quality of the complete point cloud generated by Poisson disk sampling is higher than that of uniform sampling.

f) **ShapeNet-ViPC [8]:** ShapeNet-ViPC is built upon ShapeNetRendering [98], aiming to assist researchers in simulating defects related to ViPC tasks and evaluating the performance of proposed methods. The dataset consists of 38,328 objects from 13 categories, including airplanes, benches, cabinets, cars, chairs, monitors, lamps, speakers, firearms, sofas, tables, cellphones, and watercraft. For each object, two types of incomplete point clouds (with or without noise) are generated from 24 different view points. The view point setting used is the same as that in ShapeNetRendering [98], 3D-R2N2 [105], PointSetGeneration [106], and Pixel2Mesh [107]. Additionally, 2,048 points are uniformly sampled from the mesh surface of each object under the corresponding view point setting to create the ground-truth complete point cloud. The image data utilizes the same 24 rendered views as ShapeNetRendering. In total, ShapeNet-ViPC contains 38,328 $\times$ 24 = 919,872 sets of training data.

2) Real World LiDAR Remote Sensing Datasets:

a) **KITTI [99]:** The acquisition device of KITTI is equipped in the vehicle with two gray-scale cameras, two color cameras, one Velodyne 3D laser scanner, and a GPS navigation system to provide a large number of real scene datasets. These scenes include real image data collected from urban areas, rural areas, and highways. Each image contains up to 15 cars and 30 pedestrians, with various degrees of occlusion and interception. The entire dataset consists of 389 pairs of stereo and optical flow images, 39.2 km visual odometry sequence, and more than 200k 3D annotated object images, which are sampled and synchronized at a frequency of 10 Hz. In general, the original dataset is divided into five categories: 'Road', 'City', 'Residential', 'Campus', and 'Person'. For 3D object detection, the label is subdivided into 8 categories: 'Car', 'Van, 'Truck', 'Pedestrian', 'Person (sitting)', 'Cyclist', 'Tram', and 'Misc'. This dataset provides benchmark tests for tasks such as stereo, optical flow, visual odometry, and 3D object detection. However, the local point clouds in this data set are highly sparse, and some point clouds have no ground truth.

b) **TUM-MLS-2016 [100]:** TUM-MLS-2016 includes a semantic labeled baseline dataset and two test data datasets for instance segmentation and annotated single 360-degree laser scans. Fig. 5 is an example of a scene in the TUM-MLS-6 dataset, from top to bottom, (a) represents the real scenes of the TUM main entrance, (b) represents MLS point cloud with intensities measured by the laser scanners, (c) represents MLS point cloud colored with respect to height, (d) represents annotated point clouds with eight different semantic labels. The dataset was collected by Dual Velodyne HDL-64E sensors at the city campus of the Technical University of Munich. The data covered about a kilometer of urban roads, with eight types of objects and more than 40 million annotated points manually marked. As a dataset for MLS, it provides a single instance of different kinds of semantic tags and related objects, and covers both measured runtime and real-time street views.

c) **Semantic3D [101]:** Semantic3D provides a large 3D point cloud dataset annotated in real scenes, with a total of over 4 billion points. It includes a variety of different urban scenes: churches, streets, railway tracks, squares, villages, soccer fields, castles, and more. The provided point clouds are obtained from state-of-the-art static scanning devices,

This work is licensed under a Creative Commons Attribution-NonCommercial-NoDerivatives 4.0 License. For more information, see https://creativecommons.org/licenses/by-nc-nd/4.0/

This article has been accepted for publication in IEEE Journal of Selected Topics in Applied Earth Observations and Remote Sensing. This is the author's version which has not been fully edited. content may change prior to final publication. Citation information: DOI 10.1109/JSTARS.2024.3362476

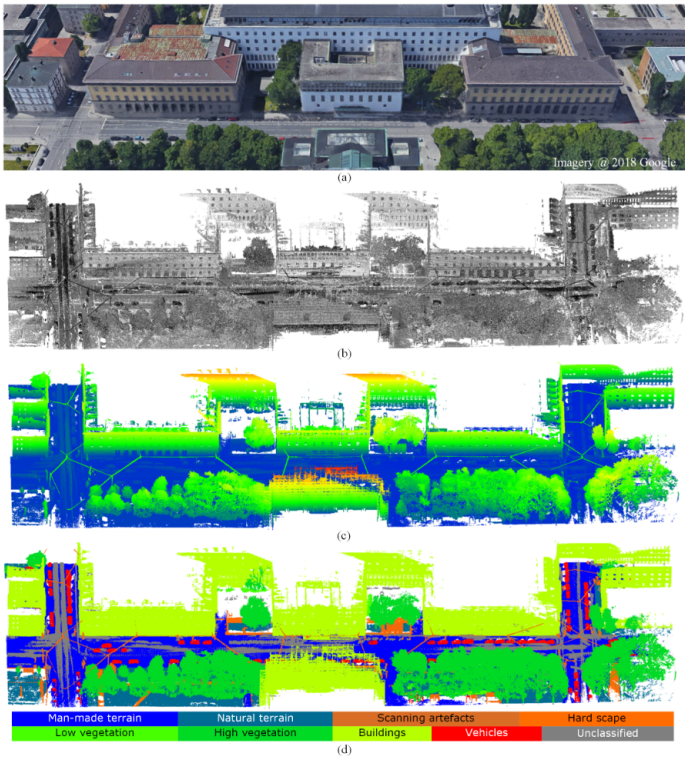


Fig. 5. A small example area of the benchmark dataset for semantic labeling. [100]

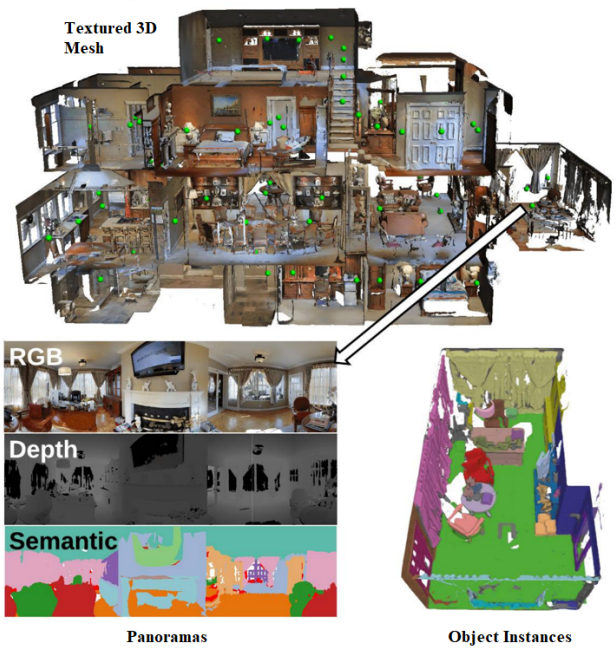


Fig. 6. Example of a MatterPort3D dataset scenario. [104]

containing very fine details. The goal of the provider is to help methods with high data demands (such as deep neural networks) to fully unleash their capabilities, enabling them to learn richer 3D representations than ever before.

d) **2D-3D-S dataset [102]:** The 2D-3D-S dataset offers a diverse range of mutually registered modalities across 2D, 2.5D, and 3D domains, complete with instance-level semantic and geometric annotations. Encompassing over 6,000 m2, the dataset comprises more than 70,000 RGB images, accompanied by corresponding depths, surface normals, semantic annotations, global XYZ images (in both regular and 360° equirectangular formats), and comprehensive camera information. Additionally, it includes registered raw and semantically annotated 3D meshes and point clouds. Furthermore, the dataset encompasses raw RGB and Depth imagery, along with associated camera information for each scan location. This dataset facilitates the development of joint and cross-modal learning models and potentially enables the implementation of unsupervised approaches that leverage the regularities inherent in large-scale indoor spaces.

e) **ScanNet [103]:** ScanNet is an RGB-D video dataset, which contains 1,513 scenes (1,201 and 312 of these scenes are used for training and testing), 2.5 million views, 21 types of objects, annotated 3D camera pose, surface reconstruction, and Instance-level semantic segmentation. Using these data helps to achieve the most advanced performance on some 3D scene understanding tasks, including 3D object classification, semantic voxel annotation, and CAD model retrieval.

f) **MatterPort3D [104]:** An RGB-D database containing a large number of complete indoor scenes. This dataset contains 194,400 RGB-D images, 10,800 panoramic images, and 24,727,520 texture triangles inside 90 buildings. At the same time, the corresponding color map, depth map, panoramic sky box, texture grid, area layout, category, and semantic segmentation are given. The annotations are surface reconstructions, camera poses, and 2D and 3D semantic segmentation. The collected 3D instance-level semantic annotations, including a total of 50,811 object instance annotations, are integrated into 40 object categories and mapped to the WordNet synset. Fig. 6 shows a scenario in a dataset that includes RGB data, depth data, and semantic data, which correspond to the room model on the right. In Textured 3D mesh, the green dots represent sampling points. The point cloud in this dataset is uneven, contains noise and holes, and needs to be completed and reconstructed.

B. Metrics

Assuming that PC_1 represents the ground truth point clouds and PC_2 represents the generated point clouds, the following three methods are commonly used to evaluate the distance between two point cloud sets.

1) Chamfer Distance: The Chamfer distance (CD) [108] describes that for each point in PC_1, find the closest point in PC_2 to this point in PC_1 and calculate the distance between the two points. Conversely, for each point in PC_2, find the point in PC_1 that is closest to this point in PC_2 and then calculate the distance between the two points, as shown in the following formula:

$$CD\left(PC_1, PC_2\right) = \frac{1}{|PC_1|} \sum_{x \in PC_1} \min_{y \in PC_2} \|x - y\|_2^2 + \frac{1}{|PC_2|} \sum_{y \in PC_2} \min_{x \in PC_1} \|y - x\|_2^2 \quad (1)$$

This work is licensed under a Creative Commons Attribution-NonCommercial-NoDerivatives 4.0 License. For more information, see https://creativecommons.org/licenses/by-nc-nd/4.0/

This article has been accepted for publication in IEEE Journal of Selected Topics in Applied Earth Observations and Remote Sensing. This is the author's version which has not been fully edited and content may change prior to final publication. Citation information: DOI 10.1109/JSTARS.2024.3362476

where x represents a point in the ground truth PC_1, and y represents a point in the generated point clouds PC_2. The calculation complexity of CD is relatively simple, and the calculation time is relatively short. CD does not require that the number of point clouds of two point cloud sets is the same. Even if the size of two point cloud sets is different, it can also be used to measure the distance between two point cloud sets. However, the work in [109] shows that it is very sensitive to outliers.

2) Earth Mover's Distance: Earth mover's distance (EMD) [108] calculates the distance between two point cloud sets with the same number, that is, the number of point clouds in PC_1 and PC_2 must be the same. EMD calculates the distance between each pair of associated points between two point cloud sets. In the calculation process, the points in the two point cloud sets have a one-to-one correspondence.

$$EMD\left(PC_1, PC_2\right) = \min_{\phi: PC_1 \to PC_2} \frac{1}{|PC_1|} \sum_{x \in PC_1} \|x - \phi(x)\|_2 \tag{2}$$

where ϕ is a bijection between ground truth point cloud set PC_1 and generated point clouds set PC_2. However, it suffers from high computational cost to find ϕ. Additionally, EMD is more discriminative to the density distribution [110].

3) Hausdorff Distance: Typically, the Hausdorff distance (HD) is used to describe the distance between different subsets of space. It converts the nonempty subset of the metric space itself into a metric space, and in simple terms, if each point of a geometry is close to its counterpart in another set, then the two sets are close at the HD. This index is compared with the mean distance in the [111] to evaluate the results of surface reconstruction. HD is approximated by

$$HD(PC_1, PC_2) = \max\left\{ \max_{(x,y)\in PC_1} |x - y|, \max_{(y,x)\in PC_2} |y - x| \right\}. \tag{3}$$

4) F1-Score: The work in [109] pointed out that Chamfer distance (CD) is sometimes misleading, and we can use F1-score [112], which is a method actively used in the multi-view 3D reconstruction community. The F1-score is defined as the average value of harmonics between precision and recall, and is used to explicitly evaluate the distance between object surfaces. The formula is as follows:

$$\mathrm{F1-Score}(d) = \frac{2P(d)R(d)}{P(d) + R(d)} \tag{4}$$

$$P(d) = \frac{1}{n_{PC_2}} \sum_{r \in PC_2} \left[\min_{t \in PC_1} \|t - r\| < d \right] \tag{5}$$

$$R(d) = \frac{1}{n_{PC_1}} \sum_{t \in PC_1} \left[\min_{r \in PC_2} \|t - r\| < d \right] \tag{6}$$

where $P(d)$ and $R(d)$ denote the precision and recall for a distance threshold d, respectively. Precision is measured by calculating the percentage of the generated point cloud whose distance to the ground truth is within the specified limit. Recall measures the completeness of reconstruction by calculating the percentage of ground truth whose distance to the generated point clouds is within the specified limit. The strictness of the F-score can be controlled by changing the distance threshold d.

5) F-Score-Coverage: Yan et al. put forward the definition of completeness invariance in their work [6] , that is, under the same missing rate, the evaluation results do not change with different missing parts. Inspired by F-Score, they used Coverage (Cov) to check the integrity of the point cloud. The Cov formula is as follows:

$$Cov\left(S_{eval}, S_{GT}\right) = \frac{\left| \left\{ \arg\min_{y \in S_{GT}} d\left(x, y\right) | x \in S_{eval} \right\} \right|}{S_{GT}} \tag{7}$$

Where $d(\cdot,\cdot)$ is the distance metric using L_2, x is the point in the evaluation point cloud S_{eval}, and y is the set of points closest to x in S_{GT}. The numerator is the sum of the quantities of y, and the denominator is the number of point clouds in S_{GT}. The value of the ratio of the equation represents the degree of coverage of point cloud to ground truth. However, Cov will be maximized due to the dense coverage of the points. Therefore, Yan et al. [6] proposed F-Score-Coverage to solve this problem. The formula is as follows:

$$F\left(S_{eval}, S_{GT}\right) = \frac{2Cov(S_{eval}, S_{GT})Cov(S_{GT}, S_{eval})}{Cov(S_{eval}, S_{GT}) + Cov(S_{GT}, S_{eval})} \tag{8}$$

Both Cov and $Cov-F-Score$ have completeness invariance. However, since Cov is a comparison between two point sets, when the number of points of the two point sets is too different, or the two point sets come from different structures, the result will be unreasonable.

C. Comparative Performance of Point Cloud Completion Results

This section summarizes the results of state-of-the-art algorithms on the specified datasets. To compare the completion results fairly, we use Completion3D as the dataset with 8 categories of 2048 points. The chamfer distance is used for evaluation, as showen in Table. III. Similarly, we compare the performance of different completion algorithms under different datasets, and the results are shown in Table. IV, Table. V, Table. VI and Table. VII. These performance comparisons, combined with the algorithm timeline described above, help us better understand the relationship between updates and iterations between algorithms, and also help to find out the direction of possible future innovation.

In the Completion3d benchmark, the best-performing method in this data set is ASFM-NET. The Asymmetrical Siamese Feature Matching (ASFM) strategy has two parts. The first component is a Siamese auto-encoder neural network that maps the partial and complete input point clouds into a shared latent space, capturing detailed shape priors. The second component is an iterative refinement unit for generating a complete point cloud. It involves mapping both partial and complete input point clouds into a shared latent space to capture detailed shape priors. An iterative refinement unit is used to generate complete point cloud. The reason why ASFM-NET has such good performance is mainly due to its full use of

This work is licensed under a Creative Commons Attribution-NonCommercial-NoDerivatives 4.0 License. For more information, see https://creativecommons.org/licenses/by-nc-nd/4.0/

This article has been accepted for publication in IEEE Journal of Selected Topics in Applied Earth Observations and Remote Sensing. This is the author's version which has not been fully edited and content may change prior to final publication. Citation information: DOI 10.1109/JSTARS.2024.3362476

the Siamese auto-encoder neural network, the use of iterative refinement units, the adoption of effective training strategies, and the full consideration of issues such as data privacy and information security.

Based on the L1 Chamfer distance metric, the second-highest of the comparison method is PMP-Net++. PMP-Net++ is an improved version based on PMPNet, which achieves superior performance in point cloud completion tasks. This method has been improved in the following aspects. First, it improves the performance of point cloud completion by introducing more contextual information, including spatial information and temporal information of point clouds. Specifically, it adopts a multi-scale feature fusion method to fuse features of different scales to capture richer contextual information. Second, the method improves the network structure of PMPNet and enhances the feature extraction capabilities of the network by introducing more convolutional layers and pooling layers. PMP-Net++ uses the residual connection to effectively alleviate the gradient disappearance problem. Third, it adds data enhancement during the training process to increase the diversity of data by performing operations such as rotation, translation, and scaling on point clouds, thereby improving the generalization ability of the model. In more advanced optimization algorithms, PMP-Net++ uses more advanced optimization algorithms, such as Adam and RMSprop, during the training process. These algorithms can converge faster and achieve better performance. In experiments, PMP-Net++ achieved better performance than PMPNet and other competing methods on multiple datasets. The best-performing method is AdaPoinTr, overall first in both comprehensive and full-category evaluation. It largely improves the previous methods and establishes the new state-of-the-art. It adopts a Transformer encoder-decoder architecture for point cloud completion. To facilitate Transformers to better leverage the inductive bias about 3D geometric structures of point cloud, AdaPoinTr further devised a geometry-aware block that models the local geometric relationships explicitly. Taking a step towards more complicated and diverse situations, they developed an adaptive query generation mechanism and designing a novel denoising task during completing a point cloud. AdaPoinTr is extended to the scene-level point cloud completion scenario by designing a new geometry-enhanced semantic scene completion framework.

Testing in the CARLA and PUGAN datasets, LiUpNet [113] achieved the best performance in many comparative methods. LiUpNet uses a combination of local features and global features to achieve more accurate point cloud completion. The network structure of LiUpNet mainly consisted of three parts, local feature extractor, global feature extractor, and decoder. Decoder used multi-layer perceptron (MLP) and inverse convolution operation to combine local features and global features to generate a complete point cloud. In experiments, LiUpNet achieved excellent performance on multiple datasets, especially in challenging point cloud completion tasks such as S3DIS and ScanNet datasets. Compared with other competing methods, LiUpNet has higher accuracy and better generalization ability, as shown in Table. V, Table. VI and Table. VII. PU-GAN is a generative adversarial network (GAN)-based point cloud upsampling network designed to learn rich point distributions from the latent space and upsample on sub-patches of the object surface. The adversarial loss encourages the generator to generate more realistic point clouds, the uniformity loss encourages the generated point cloud to be evenly distributed on the surface of the target object, and the reconstructive loss encourages the generator to retain the structural information of the input point cloud. PU-GAN used self-attention units to enhance feature integration capabilities, while LiUpNet used local feature extractors and global feature extractors to extract features of point clouds. LiUpNet's features are more comprehensive, contributing to better model performance.

V. Application in Downstream Tasks

A. Classification

This section delves into the utilization of dense point cloud completion algorithms in point cloud classification. Point clouds acquired from LiDAR sensors is often missing. If it is lost, the missing point cloud can be inputted into the point cloud completion module for the quick completion processing before performing other tasks. The network structure of point cloud classification is shown in Fig. 7. In this approach, the network takes point cloud as the input and transforms it into a 3DmFV representation on a grid. The network architecture primarily consists of an Inception module, which is illustrated in Fig. 7(a), along with max-pooling layers and four fully connected layers. The output of the network is a set of classification scores. The partial point cloud signifies a limited section of the object, typically challenging to identify. In the task of point cloud object classification, a complete point cloud is generally more conducive to accurate classification. Therefore, the process of point cloud completion becomes crucial. Through point cloud completion algorithms, missing parts can be recovered from incomplete point clouds, making the point cloud more comprehensive and closer to the actual shape of the object. This contributes to improving the performance of classification models, enabling them to more accurately learn and understand the features of objects, thereby enhancing classification accuracy and robustness.

B. Segmentation

Yan et al. [126] introduced JS3C-Net, which implemented enhanced sparse single-scan LiDAR semantic segmentation by assisting scene completion. In order to better weigh performance and effectiveness, they designed auxiliary components in cascaded and one-time manner and proposed a novel point-voxel interaction (PVI) module to better achieve feature interaction and fusion between two tasks.

The pipeline of S3C-NET1 is shown in Fig. 8. Given a sparse incomplete single sweep point cloud, the sparse convolutional U-Net is first used to encode F_{enc} for point features. On the basis of initial coding, shape embedded (SE) F_{SE} is generated by MLP_1, which flows into MLP_3, and then F_{out} is generated by MLP_2, which is used for point cloud semantic segmentation. Then, the incomplete fine-grained point features from SE and the complete element features of semantic scene

This work is licensed under a Creative Commons Attribution-NonCommercial-NoDerivatives 4.0 License. For more information, see https://creativecommons.org/licenses/by-nc-nd/4.0/

This article has been accepted for publication in IEEE Journal of Selected Topics in Applied Earth Observations and Remote Sensing. This is the author's version which has not been fully edited and content may change prior to final publication. Citation information: DOI 10.1109/JSTARS.2024.3362476

TABLE III
A QUANTITATIVE COMPARISON OF 8 CATEGORIES IS PERFORMED ON THE COMPLETION3D BENCHMARK. (LOWER IS BETTER)

Methods	Chamfer Distance (10^{-4})								
	Airplane	Cabinet	Car	Chair	Lamp	Sofa	Table	Watercraft	Mean
ASFM-Net [67]	**2.38**	**9.68**	**5.84**	**7.47**	**7.11**	**9.65**	**6.25**	4.84	**6.68**
SnowflakeNet [73]	3.48	11.09	6.9	8.75	8.42	10.15	6.46	5.32	7.60
VE-PCN [41]	3.83	12.74	7.86	8.66	7.24	11.47	7.88	**4.75**	8.10
VRCNet [71]	3.94	10.93	6.44	9.32	8.32	11.35	8.60	5.78	8.12
SCRN [114]	3.35	12.81	7.78	9.88	10.12	12.95	9.77	6.10	9.13
CRN [115]	3.38	13.17	8.31	10.62	10.00	12.86	9.16	5.80	9.21
PMP-Net [69]	3.99	14.70	8.55	10.21	9.27	12.43	8.51	5.77	9.23
GRNet [40]	6.13	16.90	8.27	12.23	10.22	14.93	10.08	5.86	10.64
SA-Net [48]	5.27	14.45	7.78	13.67	13.53	14.22	11.75	8.84	11.22
3D-GCN [116]	5.27	19.02	12.51	13.32	10.94	14.11	10.73	5.90	11.55
SoftPoolNet [68]	4.89	18.86	10.17	15.22	12.34	14.87	11.84	6.48	11.90
TopNet [59]	7.32	18.77	12.88	19.82	14.60	16.29	14.89	8.82	14.25
PointNetFCAE	10.30	19.06	11.82	24.68	20.30	20.09	17.57	10.50	16.88
N-DPC [117]	10.83	21.17	13.57	22.97	19.26	19.91	16.53	10.66	16.95
SFA-Net [53]	6.52	26.60	10.83	27.86	23.21	23.58	11.66	7.41	17.34
AtlasNet [118]	10.36	23.40	13.40	24.16	20.24	20.82	17.52	11.62	17.77
HyperPocket [54]	8.60	25.34	12.18	25.08	21.31	19.81	19.76	10.44	17.91
PointSetVoting [119]	6.88	21.18	15.78	22.54	18.78	28.39	19.96	11.16	18.18
PCN [57]	9.79	22.70	12.43	25.14	22.72	20.26	20.27	11.73	18.22
FoldingNet [46]	12.83	23.01	14.88	25.69	21.79	21.31	20.71	11.51	19.07

TABLE IV
POINT CLOUD COMPLETION ON PCN DATASET IN TERM OF PER-POINT L1 CHAMFER DISTANCE $\times$ 10^3 (LOWER IS BETTER). [120]

Methods	Average	Plane	Cabinet	Car	Chair	Lamp	Couch	Table	Watercraft
FoldingNet [46]	14.31	9.49	15.8	12.61	15.55	16.41	15.97	13.65	14.99
TopNet [59]	12.15	7.61	13.31	10.90	13.82	14.44	14.78	11.22	11.12
AtlasNat [118]	10.85	6.37	11.94	10.10	12.06	12.37	12.99	10.33	10.61
PCN [57]	9.64	5.50	22.70	10.63	8.70	11.00	11.34	11.68	8.59
GRNet [40]	8.83	6.45	10.37	9.45	9.41	7.96	10.5	8.44	8.04
CRN [115]	8.51	4.79	9.97	8.31	9.49	8.94	10.69	7.81	8.05
NSFA [53]	8.06	4.76	10.18	8.63	8.53	7.03	10.53	7.35	7.48
PMP-Net [69]	8.66	5.50	11.10	9.62	9.47	6.89	10.74	8.77	7.19
PMP-Net++ [120]	7.56	4.39	9.96	8.53	8.09	6.06	9.82	7.17	6.52
PoinTr [83]	8.38	4.75	10.47	8.68	9.39	7.75	10.93	7.78	7.29
SeedFormer [85]	6.74	3.85	9.05	8.06	7.06	**5.21**	8.85	6.05	5.85
AdaPoinTr [84]	**6.53**	**3.68**	**8.82**	**7.47**	**6.85**	5.47	**8.35**	**5.80**	**5.76**

TABLE V
QUANTITATIVE RESULTS [113] ON THE CARLA [121] DATASET (OUTDOOR, LIDAR POINT CLOUD)

Methods	CD (10^{-3})	EMD (10^{-2})	HD (10^{-3})	Time cost (ms)
PU-Net [56]	3.534	4.027	28.170	10.04
MPU [122]	3.371	3.152	23.327	10.86
PU-GAN [123]	1.922	2.350	17.753	14.28
PU-GCN [124]	1.867	2.147	16.269	**8.83**
LiUpNet [113]	**1.684**	**2.017**	**13.682**	11.10

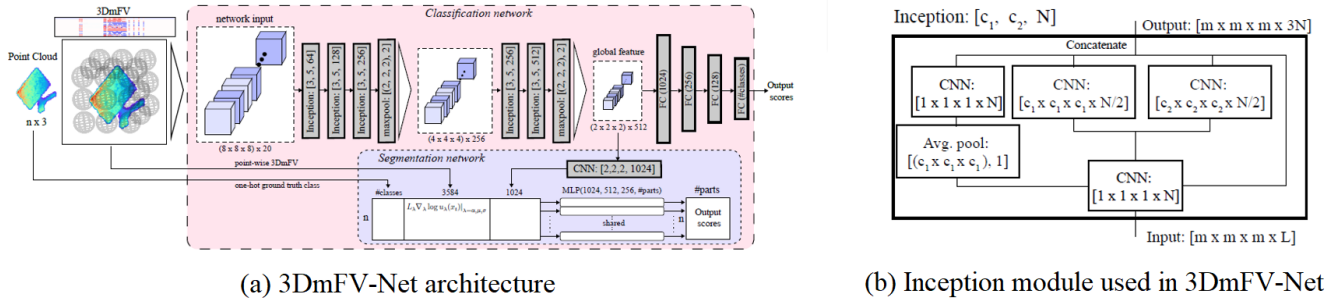
TABLE VI
QUANTITATIVE RESULTS [113] ON THE PUGAN DATASET. (LOWER IS BETTER)

Methods	CD (10^{-3})	HD (10^{-3})	Time cost (ms)
PU-Net [56]	0.520	3.952	10.04
MPU [122]	0.279	4.959	10.86
PU-GAN [123]	0.242	3.020	14.28
PU-GCN [124]	0.260	**2.919**	**8.83**
LiUpNet [113]	**0.237**	3.655	11.10

completion (SSC) module flow into the PVI module to achieve the refinement features, and finally output the complement elements under supervision. Note that, SSC and PVI modules

This work is licensed under a Creative Commons Attribution-NonCommercial-NoDerivatives 4.0 License. For more information, see https://creativecommons.org/licenses/by-nc-nd/4.0/

This article has been accepted for publication in IEEE Journal of Selected Topics in Applied Earth Observations and Remote Sensing. This is the author's version which has not been fully edited content may change prior to final publication. Citation information: DOI 10.1109/JSTARS.2024.3362476



(a) 3DmFV-Net architecture (b) Inception module used in 3DmFV-Net

Fig. 7. [125]3D convolutional neural network framework for point cloud classification and segmentation.

TABLE VII
QUANTITATIVE RESULTS ON THE PU1K DATASET. (LOWER IS BETTER)

Methods	CD (10^{-3})	HD (10^{-3})	Time cost (ms)
PU-Net [56]	1.174	16.782	10.04
MPU [122]	0.937	12.200	10.86
PU-GAN [123]	0.702	9.530	14.28
PU-GCN [124]	0.579	7.568	**8.83**
LiUpNet [113]	**0.505**	**6.262**	11.10

can be discarded during inference. In practical applications, the general attraction point cloud segmentation network is first used to perform initial point semantic segmentation and shape embedding for each incomplete single-frame point cloud. The SSC module takes the result of the segmentation network as inputs and generates a complete voxel of the entire scene through a dense CNN. At the same time, the shape perception knowledge transfer is carried out by using the proposed PVI module.

C. Object Monitoring

Xia et al. [127] proposed the VPC-Net method, whose goal is to use raw LiDAR data to provide vehicle shapes for monitoring tasks. This method makes up for the insufficiency of the Simultaneous Localization and Mapping (SLAM) monitoring technology proposed by Cadena et al. [128] in reconstructing the complete shape of the moving vehicle. It assists in recognizing the shape of the vehicle and providing complete information on the shape of the car, and then applies the obtained information in the 3D vehicle monitoring task. Xia et al. [127] placed a Velodyne HDL-64E rotating 3D laser scanner in the center of the intersection to collect dense and accurate 3D spatial information. The circular hole in Fig. 9(a) is the position of the LiDAR system. In the LiDAR-based system, a band-shaped brown point cloud is used to represent a moving car. They detect dynamic vehicles from each frame of the original data and use VPC-Net to complete the reconstruction of the complete shape of the vehicle. Fig. 9(b-e) show that a complete vehicle appears at an intersection at consecutive times T1, T2, T3, and T4. The results show that the method can be used in the real-time monitoring of 3D vehicles.

D. Robot Navigation

There are many ways to navigate mobile robots, such as inertial navigation, magnetic navigation, visual navigation, and satellite navigation. These navigation methods are suitable for a variety of different environments, including indoor and outdoor, structured and unstructured. Among them, related to the depth of point cloud, completion are visual navigation and sensor-based data navigation. In visual navigation, the robot uses the assembled camera to take local image of the surrounding environment, and performs robot positioning and route planning through image processing technology (such as feature recognition, distance estimation, etc.). Some researchers use the Fourier transformation to process the all-round image of the robot, and store the data obtained by the key position image by the Fourier transformation as the reference point for robot positioning, so that the images taken by the robot are transformed and compared with it, so as to know the current position of the robot. Some researchers also use the vision technology to calculate the collision avoidance point in the process of robot movement and then realize the local path planning of the robot. Among them, acquiring information about the position, direction and environment a mobile robot is in space by certain detection means and semantically completing incomplete information is an important part of the process of robot perception of the environment. Fig. 10 shows the robot navigating in 3D space, where the white trajectory pointed by the arrow in the red box represents the robot's path of action. From the top articles in recent years, due to the increasing maturity of pure visual SLAM technology, the research of fused SLAM for machine navigation with the help of LiDAR point clouds has received great attention. Therefore, point cloud completion work is bound to assume an important role in robot navigation research.

VI. DISCUSSION

This survey comprehensively reviewed the advancements in developing and applying point cloud completion to various downstream tasks. We summarized the remarkable results of both traditional and deep learning based point cloud completion methods. However, there are still many tasks to be explored and further improved.

This work is licensed under a Creative Commons Attribution-NonCommercial-NoDerivatives 4.0 License. For more information, see https://creativecommons.org/licenses/by-nc-nd/4.0/

This article has been accepted for publication in IEEE Journal of Selected Topics in Applied Earth Observations and Remote Sensing. This is the author's version which has not been fully edited and content may change prior to final publication. Citation information: DOI 10.1109/JSTARS.2024.3362476

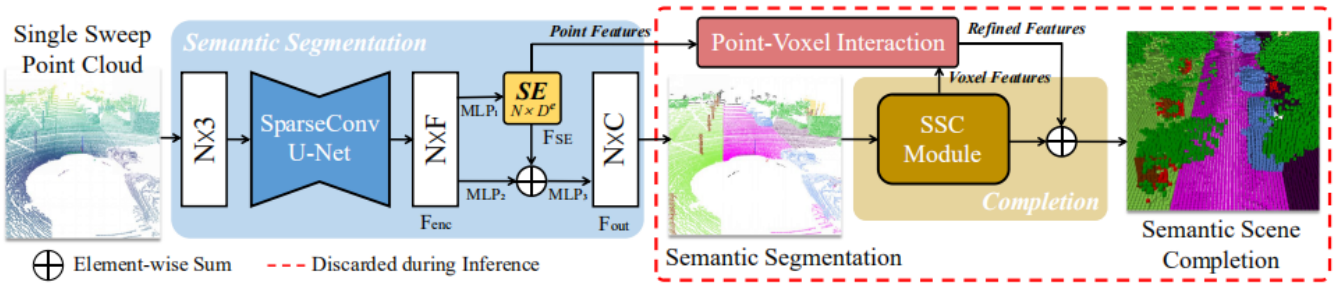


Fig. 8. JS3C-Net [126] overall pipeline.

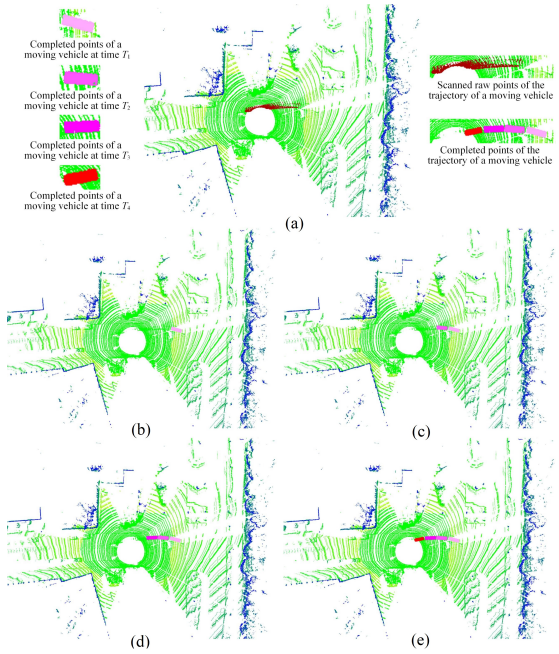


Fig. 9. Applied to 3D real-time monitoring [127]. (a) SLAM technology is used to realize the visualization of 3D traffic scenes at intersections. (b)-(d) Different colorful point clouds represent the completed point clouds by VPC-Net of this vehicle appears at different times.

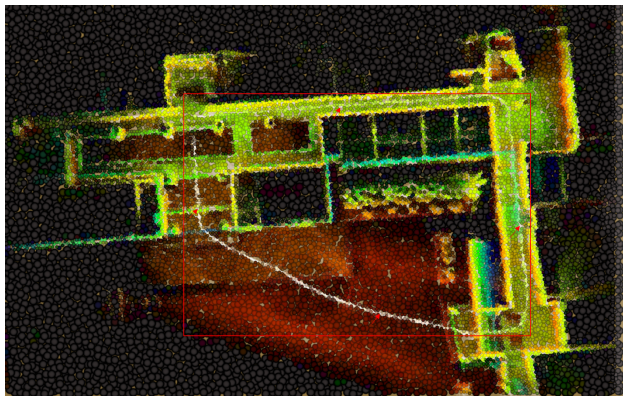


Fig. 10. Robot navigation in 3D point cloud space.

A. Limitations

Based on the above discussions, there are still some problems to be solved. The traditional geometry-based point cloud completion methods can complete the completion of the overall shapes without any external auxiliary data, using the known point cloud to remember the geometric information. However, the disadvantages of such methods are obvious, that is, more accurate point clouds must be provided, and these methods are poorly generalized and cannot be better applied to various scenarios.

Current researches are mostly focused on synthetic datasets, and applications in real-world scenarios are not yet mainstream. Therefore, to promote the rapid development and application of point cloud completion in the community, we hope that researchers can release more real-world scene data for the study of point cloud completion algorithms, including various aspects such as autonomous driving, buildings, vegetation, etc. Meanwhile, in real-world scenarios, point cloud completion relies on denoising algorithms, or the selection of algorithms with the capability to handle noisy data. In dense and uneven real point clouds, the combination of the advantages of both algorithms still needs to be explored.

B. Future Directions

The learning-based point cloud completion methods solve the problem of poor generalization of traditional completion methods and effectively achieve feature extraction and generation by using the encoding-decoding network structure. In the current case, learning-based methods have dominated and are very effective in complementing point cloud models for most objects. It is worth noting that point cloud completion will play a more important role in the face of remote sensing application scenarios such as environment perception, autonomous driving, and virtual geographic environments, and it may be necessary to focus on the lightweight and real-time nature of point cloud completion in the future. We call for a thorough consideration of discussions on computational time and resource utilization in the application of point cloud completion within the remote sensing community, and encourage its inclusion in publications.

Current point cloud completion algorithms based on GANs have achieved outstanding results but rely on guiding with random noise and conditional variables. In contrast, diffusion models are able to describe facts more accurately and exhibit better stability. At the same time, multi-modal research is rapidly advancing in the field of remote sensing, involving

This work is licensed under a Creative Commons Attribution-NonCommercial-NoDerivatives 4.0 License. For more information, see https://creativecommons.org/licenses/by-nc-nd/4.0/

This article has been accepted for publication in IEEE Journal of Selected Topics in Applied Earth Observations and Remote Sensing. This is the author's version which has not been fully edited and content may change prior to final publication. Citation information: DOI 10.1109/JSTARS.2024.3362476

strategies such as using images and natural language to assist in point cloud analysis. Explain the completion results using extra inputs and outputs may be able to develop for model explainability. Therefore, exploring the role and applications of multi-modal approaches in point cloud completion is also a future development direction.

VII. Conclusion

Point cloud completion plays an important role in a series of remote sensing applications such as autonomous driving, and virtual geographic environments, aiming at accurately predicting the missing parts for mutilated 3D point clouds. In this survey, we systematically review and summarize the traditional and deep learning based point cloud completion methods, and provide a comprehensive performance comparison of these methods. Meanwhile, the superiority and shortcomings of each method are analyzed. In addition, this survey also briefly discusses the remote sensing applications of 3D point clouds, and tries to describe the future research directions. The development of point cloud completion work is in full swing. Especially in the last three years, this field has achieved abundant research results. We are optimistic about future developments and opportunities. Especially with the arrival of large language models, 3D point cloud feature alignment with text and completion through fine-tuning of large models will be the future research direction.

Acknowledge

The authors would like to thank the National Natural Science Foundation of China under Grant 42371343, and Guangdong Basic and Applied Basic Research Natural Science Funding Schemes. We also appreciate the valuable comments and constructive suggestions from the anonymous reviewers that helped improve the manuscript.

References

[1] B. Zhao, X. Chen, X. Hua, W. Xuan, and D. D. Lichti, "Completing point clouds using structural constraints for large-scale points absence in 3d building reconstruction," *ISPRS Journal of Photogrammetry and Remote Sensing*, vol. 204, pp. 163–183, 2023. 2

[2] J. Xu, Z. Wan, and J. Wei, "Learning contours for point cloud completion," *Remote Sensing*, vol. 15, no. 17, p. 4338, 2023. 2

[3] X. Wen, Z. Han, Y.-P. Cao, P. Wan, W. Zheng, and Y.-S. Liu, "Cycle4completion: Unpaired point cloud completion using cycle transformation with missing region coding," *arXiv preprint arXiv:2103.07838*, 2021. 9

[4] C. R. Qi, H. Su, K. Mo, and L. J. Guibas, "Pointnet: Deep learning on point sets for 3d classification and segmentation," in *Proceedings of the IEEE conference on computer vision and pattern recognition*, 2017, pp. 652–660. 2, 7

[5] C. R. Qi, L. Yi, H. Su, and L. J. Guibas, "Pointnet++: Deep hierarchical feature learning on point sets in a metric space," in *Advances in neural information processing systems*, 2017, pp. 5099–5108. 2, 7

[6] W. Yan, R. Zhang, J. Wang, S. Liu, T. H. Li, and G. Li, "Vaccine-stylenet: Point cloud completion in implicit continuous function space," in *Proceedings of the 28th ACM International Conference on Multimedia*, 2020, pp. 2067–2075. 3, 9, 13

[7] C. Xie, C. Wang, B. Zhang, H. Yang, D. Chen, and F. Wen, "Style-based point generator with adversarial rendering for point cloud completion," *arXiv preprint arXiv:2103.02535*, 2021. 3, 8

[8] X. Zhang, Y. Feng, S. Li, C. Zou, H. Wan, X. Zhao, Y. Guo, and Y. Gao, "View-guided point cloud completion," in *Proceedings of the IEEE/CVF Conference on Computer Vision and Pattern Recognition*, 2021, pp. 15 890–15 899. 3, 10, 11

[9] J. Zhang, X. Chen, Z. Cai, L. Pan, H. Zhao, S. Yi, C. K. Yeo, B. Dai, and C. C. Loy, "Unsupervised 3d shape completion through gan inversion," in *Proceedings of the IEEE/CVF Conference on Computer Vision and Pattern Recognition*, 2021, pp. 1768–1777. 3, 9

[10] M. Liu, L. Sheng, S. Yang, J. Shao, and S.-M. Hu, "Morphing and sampling network for dense point cloud completion," in *Proceedings of the AAAI Conference on Artificial Intelligence*, vol. 34, no. 07, 2020, pp. 11 596–11 603. 3, 8

[11] M. Kazhdan, M. Bolitho, and H. Hoppe, "Poisson surface reconstruction," in *Proceedings of the fourth Eurographics symposium on Geometry processing*, vol. 7, 2006. 3

[12] M. Kazhdan and H. Hoppe, "Screened poisson surface reconstruction," *ACM Transactions on Graphics (ToG)*, vol. 32, no. 3, pp. 1–13, 2013. 4

[13] W. Zhao, S. Gao, and H. Lin, "A robust hole-filling algorithm for triangular mesh," *The Visual Computer*, vol. 23, no. 12, pp. 987–997, 2007. 4

[14] L. Yang, Q. Yan, and C. Xiao, "Shape-controllable geometry completion for point cloud models," *Vis. Comput.*, vol. 33, no. 3, pp. 385–398, 2017. [Online]. Available: https://doi.org/10.1007/s00371-016-1208-1 4

[15] Z. Cai, C. Wang, C. Wen, and J. Li, "3d-patchmatch: An optimization algorithm for point cloud completion," in *2015 2nd IEEE International Conference on Spatial Data Mining and Geographical Knowledge Services (ICSDM)*. IEEE, 2015, pp. 157–161. 4

[16] R. Schnabel, P. Degener, and R. Klein, "Completion and reconstruction with primitive shapes," in *Computer Graphics Forum*, vol. 28, no. 2. Wiley Online Library, 2009, pp. 503–512. 4

[17] Y. Li, X. Wu, Y. Chrysathou, A. Sharf, D. Cohen-Or, and N. J. Mitra, "Globfit: Consistently fitting primitives by discovering global relations," in *ACM SIGGRAPH 2011 papers*, 2011, pp. 1–12. 4

[18] R. Schnabel, R. Wahl, and R. Klein, "Efficient ransac for point-cloud shape detection," in *Computer graphics forum*, vol. 26, no. 2. Wiley Online Library, 2007, pp. 214–226. 4

[19] G. Li, L. Liu, H. Zheng, and N. J. Mitra, "Analysis, reconstruction and manipulation using arterial snakes," *ACM Trans. Graph.*, vol. 29, no. 6, p. 152, 2010. 4

[20] M. Kazhdan, T. Funkhouser, and S. Rusinkiewicz, "Symmetry descriptors and 3d shape matching," in *Proceedings of the 2004 Eurographics/ACM SIGGRAPH symposium on Geometry processing*, 2004, pp. 115–123. 4

[21] S. Thrun and B. Wegbreit, "Shape from symmetry," in *Tenth IEEE International Conference on Computer Vision (ICCV'05) Volume 1*, vol. 2. IEEE, 2005, pp. 1824–1831. 4

[22] N. J. Mitra, L. J. Guibas, and M. Pauly, "Partial and approximate symmetry detection for 3d geometry," *ACM Transactions on Graphics (TOG)*, vol. 25, no. 3, pp. 560–568, 2006. 5

[23] M. Pauly, N. J. Mitra, J. Wallner, H. Pottmann, and L. J. Guibas, "Discovering structural regularity in 3d geometry," in *ACM SIGGRAPH 2008 papers*, 2008, pp. 1–11. 5

[24] Q. Zheng, A. Sharf, G. Wan, Y. Li, N. J. Mitra, D. Cohen-Or, and B. Chen, "Non-local scan consolidation for 3d urban scenes," *ACM Trans. Graph.*, vol. 29, no. 4, pp. 94–1, 2010. 5

[25] I. Sipiran, R. Gregor, and T. Schreck, "Approximate symmetry detection in partial 3d meshes," in *Computer Graphics Forum*, vol. 33, no. 7. Wiley Online Library, 2014, pp. 131–140. 5

[26] P. Speciale, M. R. Oswald, A. Cohen, and M. Pollefeys, "A symmetry prior for convex variational 3d reconstruction," in *European Conference on Computer Vision*. Springer, 2016, pp. 313–328. 5

[27] L. Nan, K. Xie, and A. Sharf, "A search-classify approach for cluttered indoor scene understanding," *ACM Transactions on Graphics (TOG)*, vol. 31, no. 6, pp. 1–10, 2012. 5

[28] Y. Li, A. Dai, L. Guibas, and M. Nießner, "Database-assisted object retrieval for real-time 3d reconstruction," in *Computer Graphics Forum*, vol. 34, no. 2. Wiley Online Library, 2015, pp. 435–446. 5

[29] Y. Shi, P. Long, K. Xu, H. Huang, and Y. Xiong, "Data-driven contextual modeling for 3d scene understanding," *Computers & Graphics*, vol. 55, pp. 55–67, 2016. 5

[30] M. Pauly, N. J. Mitra, J. Giesen, M. H. Gross, and L. J. Guibas, "Example-based 3d scan completion," in *Symposium on Geometry Processing*, no. CONF, 2005, pp. 23–32. 5

[31] S. Gupta, P. Arbeláez, R. Girshick, and J. Malik, "Aligning 3d models to rgb-d images of cluttered scenes," in *Proceedings of the IEEE conference on computer vision and pattern recognition*, 2015, pp. 4731–4740. 5

This work is licensed under a Creative Commons Attribution-NonCommercial-NoDerivatives 4.0 License. For more information, see https://creativecommons.org/licenses/by-nc-nd/4.0/

This article has been accepted for publication in IEEE Journal of Selected Topics in Applied Earth Observations and Remote Sensing. This is the author's version which has not been fully edited and content may change prior to final publication. Citation information: DOI 10.1109/JSTARS.2024.3362476

[32] D. Li, T. Shao, H. Wu, and K. Zhou, "Shape completion from a single rgbd image," *IEEE transactions on visualization and computer graphics*, vol. 23, no. 7, pp. 1809–1822, 2016. 6

[33] C.-H. Shen, H. Fu, K. Chen, and S.-M. Hu, "Structure recovery by part assembly," *ACM Transactions on Graphics (TOG)*, vol. 31, no. 6, pp. 1–11, 2012. 6

[34] M. Sung, V. G. Kim, R. Angst, and L. Guibas, "Data-driven structural priors for shape completion," *ACM Transactions on Graphics (TOG)*, vol. 34, no. 6, pp. 1–11, 2015. 6

[35] Z. Wu, S. Song, A. Khosla, F. Yu, L. Zhang, X. Tang, and J. Xiao, "3d shapenets: A deep representation for volumetric shapes," in *Proceedings of the IEEE conference on computer vision and pattern recognition*, 2015, pp. 1912–1920. 6, 10, 11

[36] D. T. Nguyen, B.-S. Hua, K. Tran, Q.-H. Pham, and S.-K. Yeung, "A field model for repairing 3d shapes," in *Proceedings of the IEEE Conference on Computer Vision and Pattern Recognition*, 2016, pp. 5676–5684. 6

[37] X. Han, Z. Li, H. Huang, E. Kalogerakis, and Y. Yu, "High-resolution shape completion using deep neural networks for global structure and local geometry inference," in *Proceedings of the IEEE international conference on computer vision*, 2017, pp. 85–93. 6

[38] Z. Li, Y. Gan, X. Liang, Y. Yu, H. Cheng, and L. Lin, "Lstm-cf: Unifying context modeling and fusion with lstms for rgb-d scene labeling," in *European conference on computer vision*. Springer, 2016, pp. 541–557. 6

[39] A. Dai, C. Ruizhongtai Qi, and M. Nießner, "Shape completion using 3d-encoder-predictor cnns and shape synthesis," in *Proceedings of the IEEE Conference on Computer Vision and Pattern Recognition*, 2017, pp. 5868–5877. 6

[40] H. Xie, H. Yao, S. Zhou, J. Mao, S. Zhang, and W. Sun, "Grnet: gridding residual network for dense point cloud completion," in *European Conference on Computer Vision*. Springer, 2020, pp. 365–381. 6, 15

[41] X. Wang, M. H. Ang, and G. H. Lee, "Voxel-based network for shape completion by leveraging edge generation," in *Proceedings of the IEEE/CVF International Conference on Computer Vision*, 2021, pp. 13 189–13 198. 6, 15

[42] G. Riegler, A. Osman Ulusoy, and A. Geiger, "Octnet: Learning deep 3d representations at high resolutions," in *Proceedings of the IEEE conference on computer vision and pattern recognition*, 2017, pp. 3577–3586. 6

[43] P.-S. Wang, Y. Liu, Y.-X. Guo, C.-Y. Sun, and X. Tong, "O-cnn: Octree-based convolutional neural networks for 3d shape analysis," *ACM Transactions On Graphics (TOG)*, vol. 36, no. 4, pp. 1–11, 2017. 7

[44] P.-S. Wang, C.-Y. Sun, Y. Liu, and X. Tong, "Adaptive o-cnn: A patch-based deep representation of 3d shapes," *ACM Transactions on Graphics (TOG)*, vol. 37, no. 6, pp. 1–11, 2018. 7

[45] B. Graham, M. Engelcke, and L. Van Der Maaten, "3d semantic segmentation with submanifold sparse convolutional networks," in *Proceedings of the IEEE conference on computer vision and pattern recognition*, 2018, pp. 9224–9232. 7

[46] Y. Yang, C. Feng, Y. Shen, and D. Tian, "Foldingnet: Point cloud auto-encoder via deep grid deformation," in *Proceedings of the IEEE Conference on Computer Vision and Pattern Recognition*, 2018, pp. 206–215. 7, 15

[47] Y. Shen, C. Feng, Y. Yang, and D. Tian, "Mining point cloud local structures by kernel correlation and graph pooling," in *Proceedings of the IEEE conference on computer vision and pattern recognition*, 2018, pp. 4548–4557. 7

[48] X. Wen, T. Li, Z. Han, and Y.-S. Liu, "Point cloud completion by skip-attention network with hierarchical folding," in *Proceedings of the IEEE/CVF Conference on Computer Vision and Pattern Recognition*, 2020, pp. 1939–1948. 7, 15

[49] P. Achlioptas, O. Diamanti, I. Mitliagkas, and L. Guibas, "Learning representations and generative models for 3d point clouds," in *International conference on machine learning*, 2018, pp. 40–49. 7, 9

[50] S. Gurumurthy and S. Agrawal, "High fidelity semantic shape completion for point clouds using latent optimization," in *2019 IEEE Winter Conference on Applications of Computer Vision (WACV)*. IEEE, 2019, pp. 1099–1108. 7

[51] M. Sarmad, H. J. Lee, and Y. M. Kim, "Rl-gan-net: A reinforcement learning agent controlled gan network for real-time point cloud shape completion," in *Proceedings of the IEEE Conference on Computer Vision and Pattern Recognition*, 2019, pp. 5898–5907. 7

[52] Z. Huang, Y. Yu, J. Xu, F. Ni, and X. Le, "Pf-net: Point fractal network for 3d point cloud completion," in *Proceedings of the IEEE/CVF Conference on Computer Vision and Pattern Recognition*, 2020, pp. 7662–7670. 7

[53] W. Zhang, Q. Yan, and C. Xiao, "Detail preserved point cloud completion via separated feature aggregation," in *Computer Vision - ECCV 2020 - 16th European Conference, Glasgow, UK, August 23-28, 2020, Proceedings, Part XXV*, ser. Lecture Notes in Computer Science, A. Vedaldi, H. Bischof, T. Brox, and J. Frahm, Eds., vol. 12370. Springer, 2020, pp. 512–528. [Online]. Available: https://doi.org/10.1007/978-3-030-58595-2_31 7, 15

[54] P. Spurek, A. Kasymov, M. Mazur, D. Janik, S. Tadeja, Ł. Struski, J. Tabor, and T. Trzciński, "Hyperpocket: Generative point cloud completion," *arXiv preprint arXiv:2102.05973*, 2021. 7, 15

[55] C. Zhao, H. Lin, Y. Yan, N. Su, and S. Tian, "A complete building extraction framework for airborne laser scanning point cloud," in *2021 IEEE International Geoscience and Remote Sensing Symposium IGARSS*. IEEE, 2021, pp. 5295–5298. 7

[56] L. Yu, X. Li, C.-W. Fu, D. Cohen-Or, and P.-A. Heng, "Pu-net: Point cloud upsampling network," in *Proceedings of the IEEE Conference on Computer Vision and Pattern Recognition*, 2018, pp. 2790–2799. 8, 15, 16

[57] W. Yuan, T. Khot, D. Held, C. Mertz, and M. Hebert, "Pcn: Point completion network," in *2018 International Conference on 3D Vision (3DV)*. IEEE, 2018, pp. 728–737. 8, 10, 11, 15

[58] L. Zhao, Y. Hu, X. Yang, Z. Dou, and L. Kang, "Robust multi-task learning network for complex lidar point cloud data preprocessing," *Expert Systems with Applications*, vol. 237, p. 121552, 2024. 8

[59] L. P. Tchapmi, V. Kosaraju, H. Rezatofighi, I. Reid, and S. Savarese, "Topnet: Structural point cloud decoder," in *Proceedings of the IEEE Conference on Computer Vision and Pattern Recognition*, 2019, pp. 383–392. 8, 11, 15

[60] Y. Peng, M. Chang, Q. Wang, Y. Qian, Y. Zhang, M. Wei, and X. Liao, "Sparse-to-dense multi-encoder shape completion of unstructured point cloud," *IEEE Access*, vol. 8, pp. 30 969–30 978, 2020. 8

[61] X. Wang, M. H. Ang, and G. H. Lee, "Point cloud completion by learning shape priors," in *IEEE/RSJ International Conference on Intelligent Robots and Systems, IROS 2020, Las Vegas, NV, USA, October 24, 2020 - January 24, 2021*. IEEE, 2020, pp. 10 719–10 726. [Online]. Available: https://doi.org/10.1109/IROS45743.2020.9340862 8

[62] M. Cheng, G. Li, Y. Chen, J. Chen, C. Wang, and J. Li, "Dense point cloud completion based on generative adversarial network," *IEEE Transactions on Geoscience and Remote Sensing*, vol. 60, pp. 1–10, 2021. 8

[63] R. Zhang, W. Gao, G. Li, and T. H. Li, "Qinet: Decision surface learning and adversarial enhancement for quasi-immune completion of diverse corrupted point clouds," *IEEE Transactions on Geoscience and Remote Sensing*, vol. 60, pp. 1–14, 2022. 8

[64] L. Pan, "Ecg: Edge-aware point cloud completion with graph convolution," *IEEE Robotics and Automation Letters*, vol. 5, no. 3, pp. 4392–4398, 2020. 8

[65] Z. Han, X. Wang, Y.-S. Liu, and M. Zwicker, "Multi-angle point cloud-vae: Unsupervised feature learning for 3d point clouds from multiple angles by joint self-reconstruction and half-to-half prediction," in *2019 IEEE/CVF International Conference on Computer Vision (ICCV)*. IEEE, 2019, pp. 10 441–10 450. 8

[66] D. Zong, S. Sun, and J. Zhao, "Ashf-net: Adaptive sampling and hierarchical folding network for robust point cloud completion," in *Proceedings of the AAAI Conference on Artificial Intelligence*, vol. 35, no. 4, 2021, pp. 3625–3632. 8

[67] Y. Xia, Y. Xia, W. Li, R. Song, K. Cao, and U. Stilla, "Asfm-net: Asymmetrical siamese feature matching network for point completion," *arXiv preprint arXiv:2104.09587*, 2021. 8, 15

[68] Y. Wang, D. J. Tan, N. Navab, and F. Tombari, "Softpoolnet: Shape descriptor for point cloud completion and classification," *arXiv preprint arXiv:2008.07358*, 2020. 9, 15

[69] X. Wen, P. Xiang, Z. Han, Y.-P. Cao, P. Wan, W. Zheng, and Y.-S. Liu, "Pmp-net: Point cloud completion by learning multi-step point moving paths," in *Proceedings of the IEEE/CVF Conference on Computer Vision and Pattern Recognition*, 2021, pp. 7443–7452. 9, 15

[70] ——, "Pmp-net++: Point cloud completion by transformer-enhanced multi-step point moving paths," *IEEE Transactions on Pattern Analysis and Machine Intelligence*, vol. 45, no. 1, pp. 852–867, 2022. 9

[71] L. Pan, X. Chen, Z. Cai, J. Zhang, H. Zhao, S. Yi, and Z. Liu, "Variational relational point completion network," *arXiv preprint arXiv:2104.10154*, 2021. 9, 11, 15

This work is licensed under a Creative Commons Attribution-NonCommercial-NoDerivatives 4.0 License. For more information, see https://creativecommons.org/licenses/by-nc-nd/4.0/

This article has been accepted for publication in IEEE Journal of Selected Topics in Applied Earth Observations and Remote Sensing. This is the author's version which has not been fully edited and content may change prior to final publication. Citation information: DOI 10.1109/JSTARS.2024.3362476

[72] ——, "Variational relational point completion network for robust 3d classification," *IEEE Transactions on Pattern Analysis and Machine Intelligence*, 2023. 9

[73] P. Xiang, X. Wen, Y.-S. Liu, Y.-P. Cao, P. Wan, W. Zheng, and Z. Han, "Snowflakenet: Point cloud completion by snowflake point deconvolution with skip-transformer," in *Proceedings of the IEEE/CVF International Conference on Computer Vision*, 2021, pp. 5499–5509. 9, 15

[74] W. Zheng and Z. Han, "Snowflake point deconvolution for point cloud completion and generation with skip-transformer," *IEEE Transactions on Pattern Analysis and Machine Intelligence*, vol. 45, no. 5, 2023. 9

[75] X. Chen, B. Chen, and N. J. Mitra, "Unpaired point cloud completion on real scans using adversarial training," in *8th International Conference on Learning Representations, ICLR 2020, Addis Ababa, Ethiopia, April 26-30, 2020*. OpenReview.net, 2020. [Online]. Available: https://openreview.net/forum?id=HkgrZ0EYwB 9

[76] X. Liu, Y. Ma, K. Xu, J. Wan, and Y. Guo, "Agfa-net: Adaptive global feature augmentation network for point cloud completion," *IEEE Geoscience and Remote Sensing Letters*, vol. 19, pp. 1–5, 2022. 9

[77] L. Tan, X. Lin, D. Niu, D. Wang, M. Yin, and X. Zhao, "Projected generative adversarial network for point cloud completion," *IEEE Transactions on Circuits and Systems for Video Technology*, vol. 33, no. 2, pp. 771–781, 2022. 9

[78] Z. Cao, W. Zhang, X. Wen, Z. Dong, Y.-s. Liu, and B. Yang, "Mfm-net: Unpaired shape completion network with multi-stage feature matching," *arXiv preprint arXiv:2111.11976*, 2021. 9

[79] Y. Zhang, J. Xu, Y. Zou, P. X. Liu, and J. Liu, "Ps-net: Point shift network for 3-d point cloud completion," *IEEE Transactions on Geoscience and Remote Sensing*, vol. 60, pp. 1–13, 2022. 9

[80] Y. Xiong, W.-C. Ma, J. Wang, and R. Urtasun, "Learning compact representations for lidar completion and generation," in *Proceedings of the IEEE/CVF Conference on Computer Vision and Pattern Recognition*, 2023, pp. 1074–1083. 9

[81] H. Son and Y. M. Kim, "Saum: Symmetry-aware upsampling module for consistent point cloud completion," in *Proceedings of the Asian Conference on Computer Vision*, 2020. 9

[82] D. Stutz and A. Geiger, "Learning 3d shape completion from laser scan data with weak supervision," in *Proceedings of the IEEE Conference on Computer Vision and Pattern Recognition*, 2018, pp. 1955–1964. 10

[83] X. Yu, Y. Rao, Z. Wang, Z. Liu, J. Lu, and J. Zhou, "Pointr: Diverse point cloud completion with geometry-aware transformers," in *Proceedings of the IEEE/CVF international conference on computer vision*, 2021, pp. 12 498–12 507. 10, 15

[84] X. Yu, Y. Rao, Z. Wang, J. Lu, and J. Zhou, "Adapointr: Diverse point cloud completion with adaptive geometry-aware transformers," *arXiv preprint arXiv:2301.04545*, 2023. 10, 15

[85] H. Zhou, Y. Cao, W. Chu, J. Zhu, T. Lu, Y. Tai, and C. Wang, "Seedformer: Patch seeds based point cloud completion with upsample transformer," in *European conference on computer vision*. Springer, 2022, pp. 416–432. 10, 15

[86] M. Wodzinski, M. Daniol, D. Hemmerling, and M. Socha, "High-resolution cranial defect reconstruction by iterative, low-resolution, point cloud completion transformers," in *International Conference on Medical Image Computing and Computer-Assisted Intervention*. Springer, 2023, pp. 333–343. 10

[87] Z. Chen, F. Long, Z. Qiu, T. Yao, W. Zhou, J. Luo, and T. Mei, "Anchorformer: Point cloud completion from discriminative nodes," in *Proceedings of the IEEE/CVF Conference on Computer Vision and Pattern Recognition*, 2023, pp. 13 581–13 590. 10

[88] S. Li, P. Gao, X. Tan, and M. Wei, "Proxyformer: Proxy alignment assisted point cloud completion with missing part sensitive transformer," in *Proceedings of the IEEE/CVF Conference on Computer Vision and Pattern Recognition*, 2023, pp. 9466–9475. 10

[89] Z. Zhu, L. Nan, H. Xie, H. Chen, J. Wang, M. Wei, and J. Qin, "Csdn: Cross-modal shape-transfer dual-refinement network for point cloud completion," *IEEE Transactions on Visualization and Computer Graphics*, 2023. 10

[90] J. Zhang, H. Zhang, R. Vasudevan, and M. Johnson-Roberson, "Hyperspherical embedding for point cloud completion," in *Proceedings of the IEEE/CVF Conference on Computer Vision and Pattern Recognition*, 2023, pp. 5323–5332. 10

[91] S. Zhang, X. Liu, H. Xie, L. Nie, H. Zhou, D. Tao, and X. Li, "Learning geometric transformation for point cloud completion," *International Journal of Computer Vision*, pp. 1–21, 2023. 10

[92] M. Xu, Y. Wang, Y. Liu, T. He, and Y. Qiao, "Cp3: Unifying point cloud completion by pretrain-prompt-predict paradigm," *IEEE Transactions on Pattern Analysis and Machine Intelligence*, 2023. 10

[93] S. Hong, M. Yavartanoo, R. Neshatavar, and K. M. Lee, "Acl-spc: Adaptive closed-loop system for self-supervised point cloud completion," in *Proceedings of the IEEE/CVF Conference on Computer Vision and Pattern Recognition*, 2023, pp. 9435–9444. 10

[94] J. Shi, P. Li, X. Chen, and S. Shen, "Are all point clouds suitable for completion? weakly supervised quality evaluation network for point cloud completion," *arXiv preprint arXiv:2303.01804*, 2023. 10

[95] H. Xiao, Y. Li, W. Kang, and Q. Wu, "Distinguishing and matching-aware unsupervised point cloud completion," *IEEE Transactions on Circuits and Systems for Video Technology*, 2023. 10

[96] Y. Wu, Z. Yan, C. Chen, L. Wei, X. Li, G. Li, Y. Li, S. Cui, and X. Han, "Scoda: Domain adaptive shape completion for real scans," in *Proceedings of the IEEE/CVF Conference on Computer Vision and Pattern Recognition*, 2023, pp. 17 630–17 641. 10

[97] C. Ma, Y. Chen, P. Guo, J. Guo, C. Wang, and Y. Guo, "Symmetric shape-preserving autoencoder for unsupervised real scene point cloud completion," in *Proceedings of the IEEE/CVF Conference on Computer Vision and Pattern Recognition*, 2023, pp. 13 560–13 569. 10

[98] A. X. Chang, T. Funkhouser, L. Guibas, P. Hanrahan, Q. Huang, Z. Li, S. Savarese, M. Savva, S. Song, H. Su *et al.*, "Shapenet: An information-rich 3d model repository," *arXiv preprint arXiv:1512.03012*, 2015. 10, 11

[99] A. Geiger, P. Lenz, C. Stiller, and R. Urtasun, "Vision meets robotics: The kitti dataset," *The International Journal of Robotics Research*, vol. 32, no. 11, pp. 1231–1237, 2013. 10, 11

[100] J. Zhu, J. Gehrung, R. Huang, B. Borgmann, Z. Sun, L. Hoegner, M. Hebel, Y. Xu, and U. Stilla, "Tum-mls-2016: An annotated mobile lidar dataset of the tum city campus for semantic point cloud interpretation in urban areas," *Remote Sensing*, vol. 12, no. 11, p. 1875, 2020. 10, 11, 12

[101] T. Hackel, N. Savinov, L. Ladicky, J. D. Wegner, K. Schindler, and M. Pollefeys, "SEMANTIC3D.NET: A new large-scale point cloud classification benchmark," in *ISPRS Annals of the Photogrammetry, Remote Sensing and Spatial Information Sciences*, vol. IV-1-W1, 2017, pp. 91–98. 11

[102] I. Armeni, A. Sax, A. R. Zamir, and S. Savarese, "Joint 2D-3D-Semantic Data for Indoor Scene Understanding," *ArXiv e-prints*, Feb. 2017. 11, 12

[103] A. Dai, A. X. Chang, M. Savva, M. Halber, T. Funkhouser, and M. Nießner, "Scannet: Richly-annotated 3d reconstructions of indoor scenes," in *Proceedings of the IEEE conference on computer vision and pattern recognition*, 2017, pp. 5828–5839. 11, 12

[104] A. Chang, A. Dai, T. Funkhouser, M. Halber, M. Niessner, M. Savva, S. Song, A. Zeng, and Y. Zhang, "Matterport3d: Learning from rgb-d data in indoor environments," *arXiv preprint arXiv:1709.06158*, 2017. 11, 12

[105] C. B. Choy, D. Xu, J. Gwak, K. Chen, and S. Savarese, "3d-r2n2: A unified approach for single and multi-view 3d object reconstruction," in *Computer Vision–ECCV 2016: 14th European Conference, Amsterdam, The Netherlands, October 11-14, 2016, Proceedings, Part VIII 14*. Springer, 2016, pp. 628–644. 11

[106] H. Fan, H. Su, and L. J. Guibas, "A point set generation network for 3d object reconstruction from a single image," in *Proceedings of the IEEE conference on computer vision and pattern recognition*, 2017, pp. 605–613. 11

[107] N. Wang, Y. Zhang, Z. Li, Y. Fu, W. Liu, and Y.-G. Jiang, "Pixel2mesh: Generating 3d mesh models from single rgb images," in *Proceedings of the European conference on computer vision (ECCV)*, 2018, pp. 52–67. 11

[108] H. Fan, H. Su, and L. Guibas, "A point set generation network for 3d object reconstruction from a single image," in *2017 IEEE Conference on Computer Vision and Pattern Recognition (CVPR)*, 2017, pp. 2463–2471. 12, 13

[109] M. Tatarchenko, S. Richter, R. Ranftl, Z. Li, V. Koltun, and T. Brox, "What do single-view 3d reconstruction networks learn?" 06 2019, pp. 3400–3409. 13

[110] M. Liu, L. Sheng, S. Yang, J. Shao, and S.-M. Hu, "Morphing and sampling network for dense point cloud completion," *Proceedings of the AAAI Conference on Artificial Intelligence*, vol. 34, pp. 11 596–11 603, 04 2020. 13

[111] M. Berger, J. A. Levine, L. G. Nonato, C. T. Silva, and G. Taubin, "A benchmark for surface reconstruction," *ACM Transactions on Graphics*, vol. 32, no. 2, pp. 1–17, 2011. 13

This work is licensed under a Creative Commons Attribution-NonCommercial-NoDerivatives 4.0 License. For more information, see https://creativecommons.org/licenses/by-nc-nd/4.0/

This article has been accepted for publication in IEEE Journal of Selected Topics in Applied Earth Observations and Remote Sensing. This is the author's version which has not been fully edited and content may change prior to final publication. Citation information: DOI 10.1109/JSTARS.2024.3362476

[112] A. Knapitsch, J. Park, Q. Y. Zhou, and V. Koltun, "Tanks and temples: benchmarking large-scale scene reconstruction," *Acm Transactions on Graphics*, vol. 36, no. 4, p. 78, 2017. 13
[113] T. Y. Chen, C. C. Hsiao, and C.-C. Huang, "Density-imbalance-eased lidar point cloud upsampling via feature consistency learning," *IEEE Transactions on Intelligent Vehicles*, 2022. 14, 15, 16
[114] X. Wang, M. H. Ang Jr, and G. H. Lee, "A self-supervised cascaded refinement network for point cloud completion," *arXiv preprint arXiv:2010.08719*, 2020. 15
[115] ——, "Cascaded refinement network for point cloud completion," in *Proceedings of the IEEE/CVF Conference on Computer Vision and Pattern Recognition*, 2020, pp. 790–799. 15
[116] Z.-H. Lin, S.-Y. Huang, and Y.-C. F. Wang, "Convolution in the cloud: Learning deformable kernels in 3d graph convolution networks for point cloud analysis," in *Proceedings of the IEEE/CVF Conference on Computer Vision and Pattern Recognition*, 2020, pp. 1800–1809. 15
[117] G. Li, Y. Chen, M. Cheng, C. Wang, and J. Li, "N-dpc: Dense 3d point cloud completion based on improved multi-stage network," in *Proceedings of the 2020 9th International Conference on Computing and Pattern Recognition*, 2020, pp. 274–279. 15
[118] T. Groueix, M. Fisher, V. G. Kim, B. C. Russell, and M. Aubry, "A papier-mâché approach to learning 3d surface generation," in *Proceedings of the IEEE conference on computer vision and pattern recognition*, 2018, pp. 216–224. 15
[119] J. Zhang, W. Chen, Y. Wang, R. Vasudevan, and M. Johnson-Roberson, "Point set voting for partial point cloud analysis," *IEEE Robotics and Automation Letters*, vol. 6, no. 2, pp. 596–603, 2021. 15
[120] X. Wen, P. Xiang, Z. Han, Y. P. Cao, P. Wan, W. Zheng, and Y. S. Liu, "Pmp-net++: Point cloud completion by transformer-enhanced multi-step point moving paths," 2022. 15
[121] A. Dosovitskiy, G. Ros, F. Codevilla, A. Lopez, and V. Koltun, "Carla: An open urban driving simulator," 2017. 15
[122] Y. Wang, S. Wu, H. Huang, D. Cohen-Or, and O. Sorkine-Hornung, "Patch-based progressive 3d point set upsampling," in *2019 IEEE/CVF Conference on Computer Vision and Pattern Recognition (CVPR)*, 2019. 15, 16
[123] R. Li, X. Li, C.-W. Fu, D. Cohen-Or, and P.-A. Heng, "Pu-gan: a point cloud upsampling adversarial network," in *Proceedings of the IEEE International Conference on Computer Vision*, 2019, pp. 7203–7212. 15, 16
[124] G. Qian, A. Abualshour, G. Li, A. Thabet, and B. Ghanem, "Pu-gcn: Point cloud upsampling using graph convolutional networks," in *Computer Vision and Pattern Recognition*, 2021. 15, 16
[125] Y. Ben-Shabat, M. Lindenbaum, and A. Fischer, "3d point cloud classification and segmentation using 3d modified fisher vector representation for convolutional neural networks," *arXiv preprint arXiv:1711.08241*, 2017. 16
[126] X. Yan, J. Gao, J. Li, R. Zhang, Z. Li, R. Huang, and S. Cui, "Sparse single sweep lidar point cloud segmentation via learning contextual shape priors from scene completion," *arXiv preprint arXiv:2012.03762*, 2020. 14, 17
[127] Y. Xia, Y. Xu, C. Wang, and U. Stilla, "Vpc-net: Completion of 3d vehicles from mls point clouds," *ISPRS Journal of Photogrammetry and Remote Sensing*, vol. 174, pp. 166–181, 2021. 16, 17
[128] C. Cadena, L. Carlone, H. Carrillo, Y. Latif, D. Scaramuzza, J. Neira, I. Reid, and J. J. Leonard, "Past, present, and future of simultaneous localization and mapping: Toward the robust-perception age," *IEEE Transactions on robotics*, vol. 32, no. 6, pp. 1309–1332, 2016. 16



Zhiyang Zhi is currently pursuing his PhD in engineering at Sun Yat-Sen University. He received his master's degree from Zhengzhou University in 2022. His research interests are point cloud processing, surface reconstruction, and 3D model generation.



Ting Han is currently pursuing his Ph.D at the School of Geospatial Engineering and Science, Sun Yat-Sen University, Zhuhai, Guangdong, China. His research interests include image and point cloud processing, semantic segmentation, 3D reconstruction, deep learning theory in 3D vision, and its applications in remote sensing and GeoAI.



Yiping Chen (Senior Member, IEEE) received the Ph.D. degree in information communication engineering from the National University of Defense Technology, Changsha, China, in 2011. From 2007 to 2011, she was an Assistant Researcher with The Chinese University of Hong Kong, Hong Kong. She is currently an Associate Professor with the School of Geospatial Engineering and Science, Sun Yat-Sen University, Zhuhai, China. She has co-authored more than 80 publications, including in top remote sensing journal such as IEEE TRANSACTIONS ON GEOSCIENCE AND REMOTE SENSING, IEEE TRANSACTIONS ON INTELLIGENT TRANSPORTATION SYSTEMS, International Society for Photogrammetry and Remote Sensing (ISPRS), Journal of Photogrammetry and Remote Sensing (JPRS), and International Journal of Applied Earth Observation and Geoinformation (JAG), and in flagship Computer Vision (CV), Artificial Intelligence (AI) conferences such as IEEE Conference on Computer Vision and Pattern Recognition (CVPR), Association for the Advancement of Artificial Intelligence (AAAI), and International Joint Conference on Artificial Intelligence (IJCAI). Her main research interests include image processing, mobile LiDAR data analysis, and GeoAI.

Dr. Chen is an Associate Editor of the IEEE TRANSACTIONS ON GEOSCIENCE AND REMOTE SENSING and the Co-Chair of the ISPRS WG I/4 on LiDAR, Laser Altimetry and Sensor Integration (2022–2026).



Zhiyun Zhuang received B.S. degree in communication and information engineering from the Information Engineering University, Zhengzhou, china, in 2008, and the Ph.D. degree in Information and Communication Engineering from the National University of Defense Technology, Changsha, China, in 2016. He is currently an assistant researcher at the college of Meteorology and Oceanography, National University of Defense Technology, Changsha, China. His main research direction is the application of underwater LiDAR.



Jun Chen received the B.Eng. degree in computer science and technology from the School of Informatics, Xiamen University, Xiamen, China, in 2020, where he is currently pursuing the master's degree in electronic information with Fujian Key Laboratory Sensing and Computing for Smart Cities. His research interests include computer vision, deep learning, and information geometry.

This work is licensed under a Creative Commons Attribution-NonCommercial-NoDerivatives 4.0 License. For more information, see https://creativecommons.org/licenses/by-nc-nd/4.0/

This article has been accepted for publication in IEEE Journal of Selected Topics in Applied Earth Observations and Remote Sensing. This is the author's version which has not been fully e
content may change prior to final publication. Citation information: DOI 10.1109/JSTARS.2024.3362476



Cheng Wang (Senior Member, IEEE) received the Ph.D. degree in signal and information processing from the National University of Defense Technology, Changsha, China, in 2002. He is currently a Professor with the School of Informatics, Xiamen University, Xiamen, China, where he is the Executive Director with the Fujian Key Laboratory of Sensing and Computing for Smart Cities. He has co-authored more than 150 articles in refereed journals including IEEE TRANSACTIONS ON GEOSCIENCE AND REMOTE SENSING, Pattern Recognition, IEEE TRANSACTIONS ON INTELLIGENT TRANSPORTATION SYSTEMS, and International Society for Photogrammetry and Remote Sensing (ISPRS), Journal of Photogrammetry and Remote Sensing, and top conferences such as IEEE Conference on Computer Vision and Pattern Recognition (CVPR), Association for the Advancement of Artificial Intelligence (AAAI), International Joint Conference on Artificial Intelligence (IJCAI), IEEE International Geoscience and Remote Sensing Society (IGARSS), and ISPRS. His research interests include point cloud analysis, multi-sensor fusion, mobile mapping, and geospatial big data.



Ming Cheng (Member, IEEE) received the Ph.D. degree in biomedical engineering from Tsinghua University, Beijing, China, in 2004. He is currently a Professor with Fujian Key Laboratory of Sensing and Computing for Smart Cities, School of Informatics, Xiamen University, Xiamen, China. He has authored over 30 papers in refereed journals and conference proceedings, including IEEE GEOSCIENCE AND REMOTE SENSING LETTERS, Neurocomputing, and IEEE International Geoscience and Remote Sensing Symposium (IGARSS) and International Society for Photogrammetry and Remote Sensing (ISPRS) Proceedings. His research interests include remote sensing image processing, point cloud processing, computer vision, and machine learning.



Xinchang Zhang received the B.S. degree in cartography from the Wuhan Institute of Surveying and Mapping, Wuhan, China, in 1982, the M.S. degree in cartography from the Wuhan Technical University of Surveying and Mapping, Wuhan, in 1994, and the Ph.D. degree in resources and environmental sciences from Wuhan University, Wuhan, in 2004.

He is currently a Professor with the School of Geography and Remote Sensing, Guangzhou University, Guangzhou, China, and a Chair Professor with Henan University, Kaifeng, China. His research interests include spatial database updating, spatial data integration, and smart city.



Nannan Qin received the ph.D. degree in photogrammetry and remote Sensing from the Wuhan University, Wuhan, China, in 2019. He is currently a Lecturer of Remote Sensing and Geomatics Engineering at the Nanjing University of Information Science and Technology, Nanjing, China. His main research interests include LiDAR point clouds, 3D vision, and GeoAI.



Lingfei Ma (Member, IEEE) received the Ph.D. degree in geomatics engineering from the University of Waterloo, Waterloo, ON, Canada, in 2020. He is currently an Assistant Professor of geospatial data science with the Central University of Finance and Economics, Beijing, China. He has published more than 40 papers in refereed journals and conferences, including IEEE TRANSACTIONS ON GEOSCIENCE AND REMOTE SENSING, ISPRS Journal of Photogrammetry and Remote Sensing, IEEE TRANSACTIONS ON INTELLIGENT TRANSPORTATION SYSTEMS, IEEE TRANSACTIONS ON NEURAL NETWORKS AND LEARNING SYSTEMS, IEEE TRANSACTIONS ON INSTRUMENTATION AND MEASUREMENT, and IEEE-CVPRW. His research interests include autonomous driving, mobile laser scanning, intelligent processing of point clouds, 3-D scene modeling, and machine learning. Dr. Ma was a recipient of the 2020 National Best Ph.D. Thesis Award granted by the Canadian Remote Sensing Society. He served as a Guest Editor for the International Journal of Applied Earth Observation and Geoinformation.

This work is licensed under a Creative Commons Attribution-NonCommercial-NoDerivatives 4.0 License. For more information, see https://creativecommons.org/licenses/by-nc-nd/4.0/